J. Print Media Technol. Res. 9(2020)1
March 2020

1-2020

ISSN 2414-6250 (Online)
CODEN JPMTBI
UDC 665

Journal of Print and Media Technology Research

Scientific contributions

ISSN 2414-6250

9 772414 625001

Editor-in-Chief Gorazd Golob (Ljubljana)

Published by iarigai
www.iarigai.org
The International Association of Research Organizations for the Information, Media and Graphic Arts Industries

J. Print Media Technol. Res. 9(2020)1
March 2020
ISSN 2414-6250 (Online)
A print version is available on-demand
ISSN 2223-8905 (Print)

Journal of Print and Media Technology Research

A PEER-REVIEWED QUARTERLY

PUBLISHED BY

The International Association of Research Organizations
for the Information, Media and Graphic Arts Industries
Magdalenenstrasse 2, D-64288 Darmstadt, Germany
http://www.iarigai.org
journal@iarigai.org

A mission statement

To meet the need for a high quality scientific publishing platform in its field, the International Association of Research Organizations for the Information, Media and Graphic Arts Industries is publishing a quarterly peer-reviewed research journal.

The journal is fostering multidisciplinary research and scholarly discussion on scientific and technical issues in the field of graphic arts and media communication, thereby advancing scientific research, knowledge creation, and industry development. Its aim is to be the leading international scientific journal in the field, offering publishing opportunities and serving as a forum for knowledge exchange between all those interested in contributing to or learning from research in this field.

By regularly publishing peer-reviewed, high quality research articles, position papers, surveys, and case studies as well as review articles and topical communications, the journal is promoting original research, international collaboration, and the exchange of ideas and know-how. It also provides a multidisciplinary discussion on research issues within the field and on the effects of new scientific and technical developments on society, industry, and the individual. Thus, it intends to serve the entire research community as well as the global graphic arts and media industry.

The journal is covering fundamental and applied aspects of at least, but not limited to, the following topics:

Printing technology and related processes

- Conventional and special printing
- Packaging
- Fuel cells and other printed functionality
- Printing on biomaterials
- Textile and fabric printing
- Printed decorations
- Materials science
- Process control

Premedia technology and processes

- Colour reproduction and colour management
- Image and reproduction quality
- Image carriers (physical and virtual)
- Workflow and management

Emerging media and future trends

- Media industry developments
- Developing media communications value systems
- Online and mobile media development
- Cross-media publishing

Social impact

- Media in a sustainable society
- Environmental issues and sustainability
- Consumer perception and media use
- Social trends and their impact on media

Submissions to the Journal

Submissions are invited at any time and, if meeting the criteria for publication, will be rapidly submitted to peer-review and carefully evaluated, selected and edited. Once accepted and edited, the papers will be published as soon as possible.

Contact the Editorial office: journal@iarigai.org

Journal of Print and Media Technology Research

1-2020

March 2020

Journal of Print and Media Technology Research is listed in:

Emerging Sources Citation Index

Scopus

Index Copernicus International

PiraBase (by Smithers Pira)

Paperbase (by Innventia and Centre Technique du Papier)

NSD – Norwegian Register for Scientific Journals, Series and Publishers

Printed in Slovenia by Collegium Graphicum, d. o. o. Ljubljana

Contents

A letter from the Editor

Gorazd Golob
Editor-in-Chief
E-mail: gorazd.golob@jpmtr.org
journal@iarigai.org

The first issue of 9th volume of the Journal comes at a time when the Covid-19 pandemic was proclaimed in the world, and most of us work at home, keeping a close eye on what is happening and hoping that we, our loved ones, friends and colleagues will bypass the disease and normalize our daily lives as soon as possible. The pandemic also influenced the work of the authors, reviewers, and editors of the present issue, but the final result definitely reflects the quality and committed work of all involved.

In the first original scientific paper, the authors present a new, relatively simple but effective method of determining the contact area of paper under surface load, which is also a measure of other significant surface properties of paper. Added value to the article is the derivation of the mathematical model for determining the contact area, the modulus, and the stress–strain characteristic of the paper.

The following research paper considers the aerosol jet deposition technique as an alternative to established printing techniques, for printing with conductive silver ink. By optimizing the process and the print parameters, the resolution and quality of the prints were achieved, proving it also suitable for applications in printed electronics.

The final research paper presented is devoted to comparing infrared and Raman microscopic methods for the analysis of offset ink absorption in the paper. The advantage of Raman microscopy is demonstrated, including for the analysis of the penetration of mineral oil from printing ink into paper.

There are some changes to the Topicalities published this time. The Editor Markéta Držková (marketa.drzkova@jpmtr.org), has for the first time included a more extensive critical book review, written by Patrick Gane, a renowned expert and long-time contributor to the Journal. I hope that publishing critical reviews of important publications in the fields covered by the Journal will become an ongoing practice.

As usual, Topicalities has published news, this time dedicated mainly to patents in the field of electrically conductive inks, which also include inks and toners used in electrography, listed in the same subcategory according to international patent classification. The support from many companies in the field helping to tackle the impact of current situation is also briefly presented. A related thought of Patrick Gane was that “for those seeking access to software and systems at this extraordinary time the message is it is worth researching what is available.” I would just like to add that this statement is true also on many other occasions in our life. In addition to the aforementioned review of the book Wetting and

Spreading Dynamics, in the Bookshelf some other newer books are presented in the Bookshelf, this time mainly from the fields of colorimetry, design, textiles, lithography (for chip-making), nanomaterials and technologies, and 3D printing.

Among the authors of the presented theses, there are two who have already co-authored contributions to the International Research Conference of iarigai and in the Journal.

Arash Hakimi Tehrani successfully defended his thesis in indirect gravure printing at the Technical University of Darmstadt, Germany. The research focused on the characterization and optimization of rubber pads when printing to 3D objects and the automation of the process itself.

Araz Rajabi Abhari completed his doctoral study at Seoul National University, South Korea. He has researched coating color formulations and their influence on the final surface and mechanical properties of coated papers.

Also, Felipe Clement Fernandes completed his thesis at the Technical University of Darmstadt, Germany. He has researched security elements and forms of stochastic printed patterns, counterfeiting technology, and further identification, analysis, and validation of samples by means of image processing.

The final overview of Events is shorter than usual. Many forums, conferences, seminars, and other events have been canceled or postponed, however, some organizers have opted for online or virtual events, including ePoster sessions with online chats and discussions. Also, the 47th International Research Conference of iarigai at Clemson University in Greenville, SC, USA, planned for September 2020 was postponed, unfortunately. The authors who already submitted their extended abstracts and all other members of our community are invited to present and publish the results of their research work as original scientific or research papers in the Journal. Since 2020, the Journal is a fully open-access publication. Every submitted paper will be double-blind reviewed and edited before publication, with no charge to the authors; these aspects remain unchanged.

Many of us are now working from home to help avoid the virus and prevent Covid-19 pandemic, but it is also an opportunity to stay active as authors, reviewers, and collaborators to the Journal. Stay healthy and be active from home or from your institution if your presence there is allowed by the authorities and is safe for you.

Ljubljana, March/April 2020

JPMTR 129 | 1911
DOI 10.14622/JPMTR-1911
UDC 676.2:621.5:531.2(182)

Original scientific paper
Received: 2019-10-28
Accepted: 2020-03-25

Compressive stress–strain behavior of paper material affected by the actual contact area

Jian Chen[1]*, Edgar Dörsam*[2]*, Jann Neumann*[3] *and Simon Weißenseel*[2]

[1] School of Mechanical Engineering, Yangzhou University, Huayang Weststr. 196, 225127 Yangzhou, China
[2] Institute of Printing Science and Technology, Darmstadt University of Technology, Magdalenenstr. 2, 64289 Darmstadt, Germany
[3] Perfecta Cutting Systems GmbH, Schäfferstr. 44, 02625 Bautzen, Germany

chenjian.tud@hotmail.com
doersam@idd.tu-darmstadt.de
neumann@perfecta.de
Simon.Weissenseel@alcon.com

Abstract

The surface topography plays a very important role in the mechanical behavior of paper materials, especially for the compressive properties of thin sheet. When the surface of the cylindrical indenter is very smooth, the actual contact area under force is usually much smaller than the nominal contact area because of the surface roughness of the paper. This paper shows a method for measuring the actual contact area; with the aid of a microscope, a new approach based on image processing technique is presented to calculate the relationship between force and actual contact area. With the help of this method, the actual pressure–deformation relation and the actual modulus of paper could also be calculated. The calculation results show that there is an obvious difference between the results calculated by actual and nominal contact area. The varied trend and the values of the actual modulus are also obtained; at the beginning of the loading the actual modulus is decreasing and then close to a constant value. The universal testing machine Zwick Z050 and the optical surface topography measuring machine Sensofar Plu Neox were employed to determine not only the strength and deformation performance but also the surface roughness of specimen. Based on the obtained results the influence of carbon paper on the compressive behavior of copy paper is further discussed from different standpoints. The numerical results demonstrate the feasibility and effectiveness of the new method.

Keywords: carbon paper, copy paper, stress–strain curve, compression modulus, surface topography

1. Introduction and background

The surface topography of paper is responsible for many important paper properties, such as gloss, and printability. The measurement and characterization of the paper's surface structure is a very important task. There are many components that are used in the paper-making process. The interactions between these components are responsible for creating the properties of the paper. The paper's surface topography can range from very rough to extremely smooth, which obviously also has an influence on mechanical properties of paper materials, especially the compressive behavior.

Generally, the surface topography is rated by using smoothness or roughness (Pino and Pladellorens, 2009). Roughness plays an important role in determining how a real object will interact with its environment. A roughness value can either be calculated on a profile (line) or on a surface (area). For the profile roughness, the average roughness R_a is the most widely used parameter. For areal roughness parameters, the average areal roughness, S_a, is more common.

The measurement and characterization of surface roughness are very important not only for paper materials, but also for metal or other materials. For example, Buchner (2008, p. 118) presented a new method for evaluating the relationship between the real contact area and the normal load. The relative real contact area of an aluminum sheet under force was calculated. In the presented papers of Chen, et al. (2013; 2014), the effect of surface roughness on the nanoindentation measurements was investigated by using finite element method; the material AISI 316 L stainless steel was used in the simulation and a 3D model with seven levels of surface roughness was developed to simulate the load-displacement behavior in an indentation process.

For paper materials, the influence of surface roughness on the compressive behavior of different papers was studied by Rättö (2005), who pointed out that when compressing thin sheets, it was important to be aware of the influence of surface roughness. In the model proposed by Schaffrath and Göttsching (1991; 1992a; 1992b), the paper body was described as one internal structure and two rough surfaces, the surface topography was described as pyramid elements, and the force–deformation relationship of paper materials was derived by using the Newton formula. A new mathematical model of paper structure and paper–press interactions was introduced by Provatas and Uesaka (2003), where the effects of fiber furnish on surface structure were examined, and the factors controlling the paper–plate contact during printing were investigated. In addition, the modification of the micro-structure at various scales of the paper surface due to the calendering process was described (Vernhes, et al., 2009; Vernhes, Dubé and Bloch, 2010).

Most other studies of paper surface roughness are still focused on experimental aspects. A number of techniques are available for characterizing the topographical features of paper surfaces; four different methods were evaluated for characterizing the smoothness of the handsheet (Singh, 2008). A fast photometric stereo method, used for the determination of surface topography and reflectance was proposed (Hansson and Johansson, 2000), and the paper surface topography under compression was also studied (Teleman, et al., 2004). Furthermore, the surface topographical differences between cross machine and machine direction for the newspaper and paperboard were investigated (Alam, et al., 2011).

Preload is often used in testing a specimen, for a process when the crosshead moves to load the specimen to a specified value before a test starts. The use of preload can improve the accuracy and repeatability of results, because the initial contact area of the surface structure is not changed from zero.

According to the metrology definitions, surfaces are classified as three groups: nominal surface, actual (real) surface and measured surface. Nominal surface is the ideal surface defined by the design, and in practice this surface does not exist; actual surface is the real physical surface that limits the body; measured surface is the surface obtained by any measurement system. Normally, the stress–strain relations of most of the materials are calculated by using the nominal contact area. The difference between actual and nominal contact area is thus ignored, while actually, for contact surface, the nominal contact area A_0 and the actual contact area $A(z)$ should be very different. Therefore, not in all the situations can be neglected. The schematic diagram of the difference between nominal and actual contact areas is shown in Figure 1.

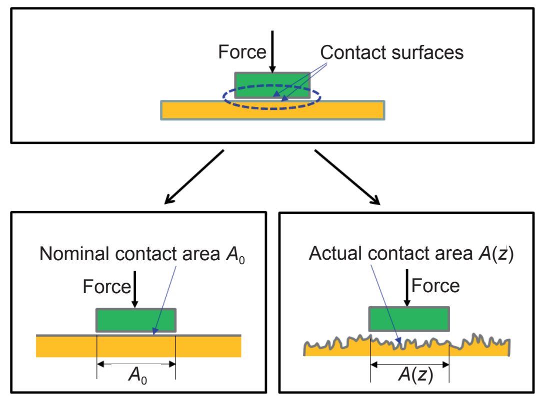

Figure 1: Schematic diagram of the difference between nominal and actual contact areas

Generally, when the indenter is very smooth, the actual contact area is much smaller than the nominal contact area because of the roughness of the paper surface. In this paper, a new experimental method for evaluating the relationship between the actual contact area and the normal load is proposed. A carbon paper is introduced in this method, and it is assumed that the measured contact areas between carbon paper and copy paper are regarded as the actual contact areas between the indenter and copy paper. Based on this assumption, the mechanical behavior of paper in through-thickness direction is discussed by deducing the actual modulus and calculating the actual stress–strain relation. Finally, the influence of the carbon paper is discussed from various aspects.

2. Materials and Methods

The copy paper (DIN A4, 80 g/m^2) selected for doing the research is produced by the Steinbeis Paper GmbH. The actual average thickness is d = 84.7 µm.

2.1 Pressure-sensitive materials

The material used here to show the contact area is carbon paper. In this research, the carbon paper Geha-1 (DIN A4, 29 g/m^2), which is produced by Geha Werke Hannover was firstly used to introduce the experimental process. The average thickness of the carbon paper Geha-1 is d = 43.6 µm. The force sensitivities of seven other different types of carbon papers were compared: SH carbon papers (SH-1, SH-2 and SH-3) produced by Shanghai Huideli Co., Ltd., DL carbon papers (DL-1, DL-2 and DL-3) produced by Deli Group Co., Ltd., and anotther carbon paper produced by Geha Werke Hannover (Geha-2), see section 3.2. The SH-1 carbon paper was selected to obtain more precise results.

Some other materials such as Fujifilm's pressure measuring film (Fujifilm, 2016) can be used to show the actual contact areas (Bachus, et al., 2006). These films can also be used for measuring the distribution of pressure (Luong, 1999, p. 66; Endres, 2006, p. 56). But in this research, Fujifilm's pressure sensitive films were not selected for measuring the distribution of pressure on copy papers, mainly because of the following two reasons.

Firstly, the Fujifilm product which can be used for measuring the low pressure is two-sheet type, which means two films (A-Film and C-Film) should be used at the same time. The maximum force used in this study was 100 N, and the contact area was around 28.27 mm^2; the ideal contact pressure thus was around 3.54 MPa, for which another type of film is suitable. On the other hand, for the very small force, for example 2 N, the pressure was only about 0.07 MPa. To keep the uniformity and correctness of the results, we cannot use three different types of films in the same test.

Secondly, considering the smaller thickness of copy paper and the surface roughness of the A-Film and C-Film, these kinds of films are not suitable to be used for the experiments described in this paper.

In the research of Endres (2006), a new pressure-sensitive film (STFI film) was developed to show the pressure distribution on the sample surface. On the one hand, the STFI film can be used for measuring the pressure range from 1 MPa to 50 MPa, but unfortunately, this film is not enough sensitive when the pressure is smaller than 1 MPa. The highest pressure used in this research was about 3 MPa, and with such a small pressure, this STFI film cannot be used to show the contact area clearly. On the other hand, the same problem as with the Fujifilm is present: the thickness of this film is 128 μm, which is more than the thickness of copy paper (84.7 μm), which would lead to big errors of the measurements.

2.2 Experimental setup

To eliminate the effect of climate conditions of the environment on the mechanical force–deformation behavior, the experimental studies were performed under standardized climatic conditions. The climate is specified in DIN 50014 and prescribed in a range of 23 ± 0.5 °C for the temperature and in a range of 50 ± 1.5 % for the relative humidity (Deutsche Institut für Normung, 2018). The samples were preliminarily treated according to DIN EN 20187 (Deutsche Institut für Normung, 1993) in order to assure an equal moisture condition in the various items delivered (Kaulitz and Dörsam, 2008).

The loading process was conducted on ZWICK Z050, which could be utilized for strain, shear and bending tests with different substrates and machine components with high accuracy of the cross head speed (0.0005–2 000 mm/min), position repetition accuracy (± 2 μm), and drive system's travel resolution (27 nm) (Kaulitz and Dörsam, 2008; Kaulitz, 2009, p. 179). The measurement device was equipped with travel sensor Heidenhain-Metro MT 2581, with the resolution of 50 nm and the repetition accuracy of 0.2 μm (Kaulitz, 2009, p. 179), produced by HEIDENHAIN GmbH. The structure of the compression device in ZWICK machine is shown in Figure 2.

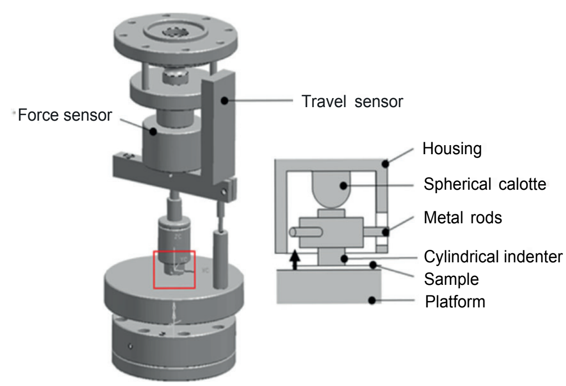

Figure 2: Test device for measuring the compressive force deformation behavior of paper (Kaulitz, 2009, p. 179)

In the device shown in Figure 2, the diameter of the cylindrical indenter is 6 mm, the area of the indenter A_{ind} is shown in Figure 3. The areal roughness of the indenter and platform could be measured by using the Sensofar PLu Neox profilometer with the objective EPI 10X-N in confocal profiling mode. The areal roughness of the indenter S_{ind} is about 385 nm and the areal roughness of the platform S_{pla} is around 650 nm. Compared with the areal roughness of paper, the S_{ind} and S_{pla} are really very small, therefore the influence from the surface roughness of indenter and platform could be ignored.

The setup of this experiment is shown in Figure 3. In order to show the actual contact areas between the indenter and copy paper, a carbon paper (Geha-1) was put above the copy paper. For carbon paper, which has two sides, only one side is the ink side; the ink side should directly be in contact with the copy paper and then the load can be imposed on the other side of carbon paper. When the force was removed, the ink of the carbon paper would be transferred on the surface of copy paper. In the following calculations, the actual contact areas between the indenter and copy paper were replaced by the measured contact areas between carbon paper and copy paper.

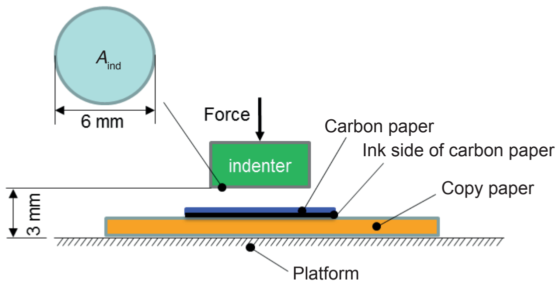

Figure 3: Experimental setup used for measuring the actual contact area

At the beginning of the loading process, the indenter moves down at the speed of 20 mm/min, until the indenter comes into contact with the surface of the carbon paper. The preload here was set as 1 N; when the change of force is 1 N, the compression process will begin at the speed of 0.05 mm/min. When the force reaches the desired maximum force, the indenter moves up at the speed of 0.05 mm/min. When the force decreases to 1 N, the indenter returns back to the original position at the speed of 20 mm/min.

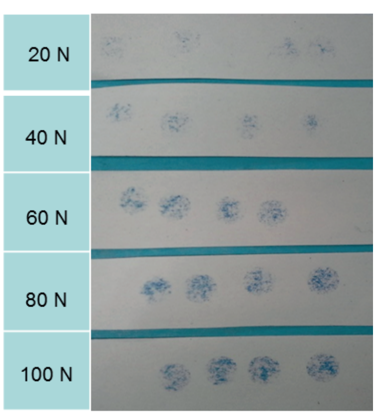

Figure 4: Measured contact areas between the carbon paper and copy paper under different forces

Five groups of preliminary experiments were carried out, the results of which are shown in Figure 4. The forces applied were 20 N, 40 N, 60 N, 80 N and 100 N. It is obvious that different forces lead to different contact areas. To improve the accuracy of the method, the force imposed in the main experiment was changing from 0 N to 100 N, with the substep of 2 N, which means 50 groups of measurements (2 N, 4 N, 6 N, 8 N,..., 96 N, 98 N, 100 N) were implemented; for each group, 20 tests were finished.

2.3 Enlarging and transferring pictures

The image processing technique was used to separate the contact area from the background. The surface of the specimen was magnified 25 times under binocular microscope and captured by a camera with resolution of 1200 × 1600 pixels. Then by the aid of MATLAB 8.1, all pictures were transformed to binary images (MATLAB help, 2013), as shown in Figure 5.

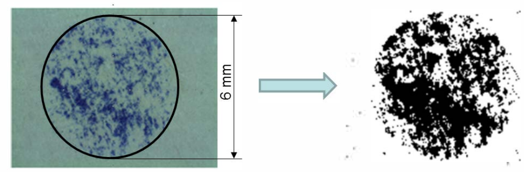

Figure 5: The example of original and binary picture

Binary images are often produced by thresholding a greyscale or color image, in order to separate an object in the image from the background. The color of the object is referred as the foreground color. The rest is referred to as the background color. MATLAB provides some methods to transform an original picture to a binary picture. The key problem here is how to determine the threshold value, as the final result is directly determined by this value. Figure 6 shows an example of the calculation results by using different threshold values. The threshold values applied here are 0.5, 0.25 and calculated by the Otsu method (Otsu, 1979). The three transformed figures are significantly different compared to the original picture, but the result of the Otsu method is the closest to the original picture (see Figure 6).

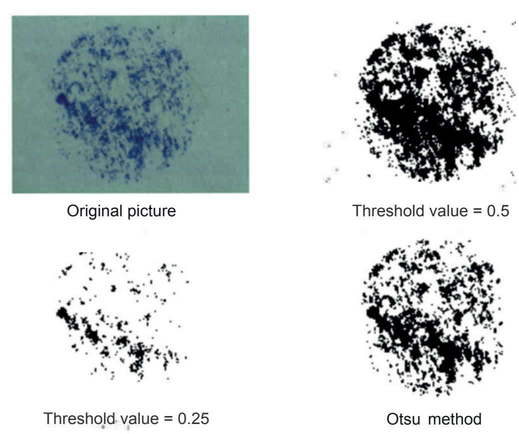

Figure 6: Examples of allpying different threshold values in transformation to a binary image

Otsu method (Otsu, 1979), named after its inventor Nobuyuki Otsu, is one of the most popular binarization algorithms. In computer vision and image processing, Otsu method is used to automatically perform clustering-based image thresholding or reduction of a gray level image to a binary image.

2.4 Calculating the contact area

For different pictures, the Otsu method will produce different threshold values. The average threshold value was calculated and used to obtain the binary images. For each of the five groups of preliminary experiments (20 N, 40 N, 60 N, 80 N, 100 N), four tests were finished (see Figure 7).

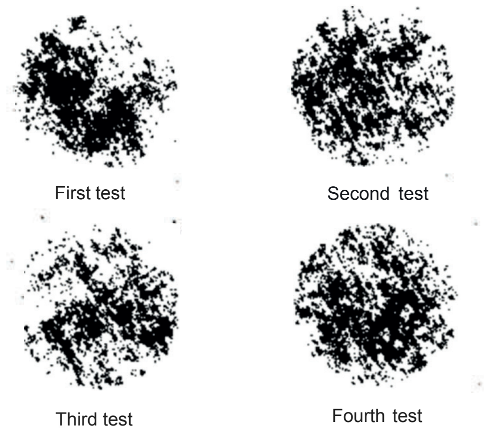

Figure 7: Example of binary images for one set of tests (Average threshold value = 0.4514, force = 100 N)

The binary pictures have resolution of 1200 × 1600 pixels, which is the same as the original pictures. The number of the pixels that belong to the black area can be calculated by using the ''bwarea'' command (MATLAB help, 2013) in MATLAB. Then, according to the proportional relation between the pixels of black area and the whole area, the value of the black area can be calculated, which is the measured contact area A_{mea}, in this paper regarded as equivalent to the actual contact area $A(z)$.

2.5 Calculating the force–contact area relation

The experiments described in section 2.2 were performed under some discrete forces. When the changes of these forces are very small, it is reasonable to assume that the deformation behavior of the material under small forces accord with the theory of elasticity. Hooke's law is the law of elasticity E under small deformation, stating that, for relatively small deformations of an object, the displacement or the size of the deformation is directly proportional to the deforming force or load. Hooke's law (Equation [1]) can also be expressed in terms of stress (σ) and strain (ε). According to Hooke's Law:

$$\sigma = \frac{E \cdot A_0}{l_0} \cdot z = E \cdot \varepsilon \Leftrightarrow F \qquad [1]$$

where A_0 is the nominal contact area, l_0 is the original length or thickness of the material, and z is the deformation under the force F.

For paper structure, the force–deformation relation can be expressed as follows:

$$F(z) = \frac{E(z) \cdot A(z)}{d} \cdot z \qquad [2]$$

with $E(z)$ being the actual modulus, which is changing with the discrete force $F(z)$, and $A(z)$ being the actual contact area, which is the discrete area calculated by the method described above, and d being the original thickness of paper.

The actual modulus of paper under different forces could be expressed as the product of actual contact pressure, paper thickness and the inverse of the total deformation.

$$E(z) = \frac{F(z)}{A(z)} \cdot \frac{1}{z} \cdot d = W(z) \cdot \frac{1}{z} \cdot d \qquad [3]$$

where:

$$W(z) = \frac{F(z)}{A(z)} \qquad [4]$$

is the actual contact pressure.

All the variable values needed here could be obtained from the implemented experiments. This method can only be used for small deformation under discrete forces.

3. Results

In this part, a simple method by using the Geha-1 carbon paper is firstly introduced to show the contact areas. Then, after comparing the sensitivities of dif-

Table 1: Experimental results of the measured contact areas under different forces with Geha-1 carbon paper

Force (N)	First test (mm^2)	Second test (mm^2)	Third test (mm^2)	Fourth test (mm^2)	Average (mm^2)	Standard deviation (mm^2)
20	3.277	3.545	3.545	3.214	3.395	0.003
40	5.811	5.885	5.503	4.521	5.430	0.011
60	9.601	10.475	9.527	9.013	9.654	0.011
80	10.269	11.508	9.379	12.610	10.941	0.025
100	10.909	13.015	12.621	13.209	12.438	0.018

ferent carbon papers as well as Fujifilm materials, a more precise method by using the SH-1 carbon paper is implemented to show the contact areas.

3.1 Preliminary calculation of the stress–strain curve of paper

In the preliminary experiments, the measured contact areas under different forces (20 N, 40 N, 60 N, 80 N, 100 N) were calculated. The results of the measured contact areas with standard deviation are shown in Table 1 and Figure 8.

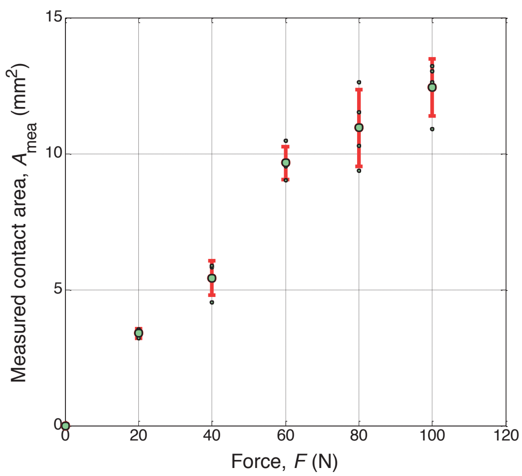

Figure 8: Measured contact areas under different forces with Geha-1 carbon paper; the error bar represents the average (mean) value and the standard deviation

The average values of each group are also plotted in Figure 9 as the discrete points. Then, the values of measured contact areas under other forces can be calculated by using the quadratic curve fitting method.

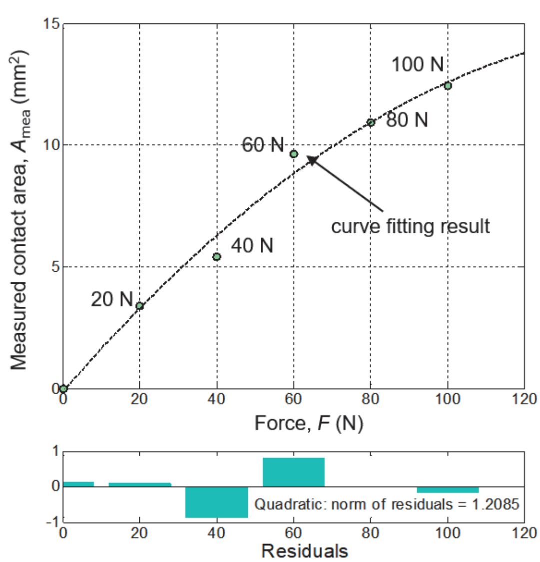

Figure 9: Measured contact areas under different forces with Geha-1 carbon paper, with quadratic curve

In Figure 9, the quadratic curve fitting method was used in the first graph. The second graph shows the corresponding residuals. The dashed black line is the fitting curve of these discrete values. The fitting function is provided as Equation [5].

$$A_{med} = 5.56 \cdot 10^{-4} \cdot F^2 + 0.183 \cdot F - 0.127 \quad [5]$$

For this curve fitting function, the norm of residuals is equal to 1.209 and the coefficient of determination is R^2 = 0.988. The calculation results show that this method can be well used to calculate the measured (actual) contact area A_{mea} ($A(z)$) under different forces $F(z)$, as well as the relationship between force and actual contact area.

According to Equation [4] and the calculation results obtained in Figure 9, the actual pressure $W(z)$ can be calculated. The values are listed in Table 2.

Table 2: Experimental (z, A) and calculation (W) results of the deformation, contact area, and actual pressure for Geha-1 carbon paper

$F(z)$(N)	**0**	**20**	**40**	**60**	**80**	**100**
z (μm)	0	3.66	5.68	7.26	8.62	9.78
$A(z)$ (mm²)	0	3.40	5.43	9.65	10.94	12.44
$W(z)$ (N·mm⁻²)	0	5.89	7.37	6.22	7.31	8.04

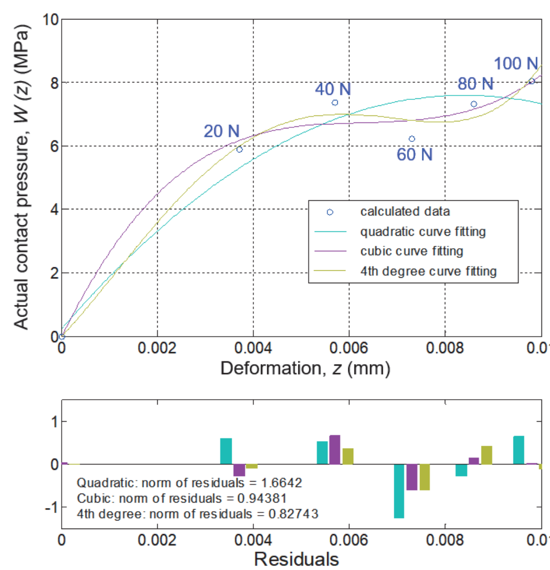

Figure 10: Relationship between the actual contact pressure and the deformation of copy paper for Geha-1 carbon paper

Here some discrete contact pressure values under different forces were obtained. The values of force $F(z)$ and the deformation z were directly obtained by Zwick machine. The values of the actual contact area $A(z)$

and the actual contact pressure $W(z)$ were obtained by the new experimental method and Equation [4]. With the method of curve fitting, the relationship between actual contact pressure $W(z)$ and deformation z was calculated and shown in Figure 10.

Three different curve fitting methods were used, the functions of which are provided in Equation [6].

Quadratic curve fitting:

$$W(z) = -0.105 \cdot z^2 + 1.76 \cdot z + 0.243 \qquad [6]$$

Cubic curve fitting:

$$W(z) = 0.0265 \cdot z^3 - 0.499 \cdot z^2 + 3.16 \cdot z - 0.029$$

4th degree curve fitting:

$$W(z) = 5.22 \cdot 10^{-3} \cdot z^4 - 0.0829 \cdot z^3 + 0.227 \cdot z^2 + 1.66 \cdot z - 6.41 \cdot 10^{-3}$$

Comparisons of corresponding residuals between different curve fitting methods are shown in the second part of Figure 8, which are used to see whether the lines are good fit for the discrete data. Both the quadratic (R^2 = 0.936), cubic (R^2 = 0.980) and 4th degree (R^2 = 0.985) curve fitting methods could be used for describing the trend of the calculated data. The residual values of cubic and 4th degree curve fitting are much smaller than the quadratic curve fitting. From the view of physical properties, no matter by using which kinds of curve fitting methods, the stress-strain–curve of paper with considering the surface roughness is very similar to the general elastic-plastic materials (Tournier, 2003). Further in this paper, cubic curve fitting method was chosen for describing the actual stress–strain curve.

When the force is changing from 0 N to 20 N, the deformation of the paper is nearly 4 µm; when the force is changing from 20 N to 100 N, the deformation of paper is only 6 µm. At the beginning of the contact, a small change in force leads to a large change in deformation. Compared with the internal structure with hard fibers, the surface structure of the paper is much easier to be compressed. When the thickness of the paper is very thin, the influence of surface roughness on the compressive response is very important and cannot be neglected.

According to Equation [3] and Table 2, the actual modulus $E(z)$ of paper under different forces can be calculated, by using the quadratic curve fitting method (see Equation [7]). The numerical trend can be described. Figure 11 shows the relationship between the actual modulus and the strain. The blue curve is the corresponding curve fitting result (see Equation [7]), R^2 = 0.954. When the force is changing from 20 N to 100 N, the actual modulus of paper is decreasing from 136 MPa to around 70 MPa.

$$E(z) = 1.77 \cdot 10^6 \cdot z^2 - 3.53 \cdot 10^4 \cdot z + 244.6 \qquad [7]$$
$$z = 0.0847 \cdot \varepsilon$$

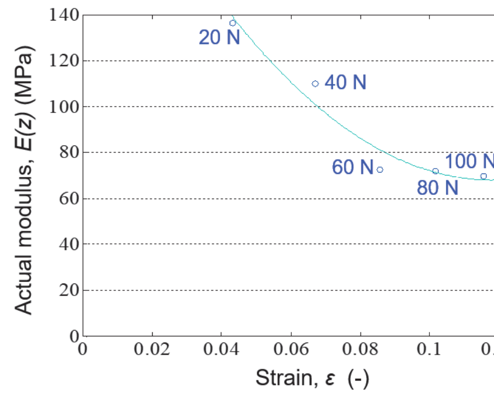

Figure 11: Stress–strain relationship of copy paper

Generally, the behavior of paper in the in-plane direction could be regarded as the elastic-plastic behavior (Xia, Boyce and Parks, 2002). But the modulus of paper material in the out-of-plane is not a constant value, which cannot be simply described by using the *E*-modulus (Mark, et al., 2001). The modulus of wood materials is considered to range from about 10 MPa to 25 GPa (Drexler, 2009); unfortunately, only very few researches discussed the modulus of paper in the out-of-plane direction. The modulus of paper in the in-plane direction is much bigger than the modulus in the out-of-plane direction. For example, the *E*-modulus of paperboard provided by Xia, Boyce and Parks (2002) in machine direction is about 5.6 GPa, and in cross machine direction is about 2.0 GPa, while the initial modulus in the out-of-plane direction is 18 MPa. The initial *E*-modulus of another paperboard in the out-of-plane measured by Stenberg (2003) is 34 MPa, and the *E*-modulus of this paperboard for fully compacted solid is about 5 GPa.

Based on the above findings, it can be seen that the calculation results of the actual modulus are reasonable. At the beginning of the compression process, the actual modulus of paper is decreasing because of the surface roughness, with the contact area approaching to the maximum contact area (approximately equal to the nominal contact area A_0), the actual modulus will be decreased to a constant value.

Figure 12 unfolds a clear comparison between the stress–strain curves of paper calculated by different methods. The compressive behavior of paper under actual contact area is very different from the result calculated by using the nominal contact area.

For the actual stress–strain curve, at the beginning of the loading process, the stiffness of paper increases with the increasing load and the relationship between stress and strain is nearly linear (or very close to linear), especially when the force is smaller than 20 N, but after that the stiffness decreases with increasing load, which is very similar to other elastic-plastic materials. For the nominal stress–strain curve, the loading process shows a typical J-shaped curve. The calculation method of the contact area plays a very important role.

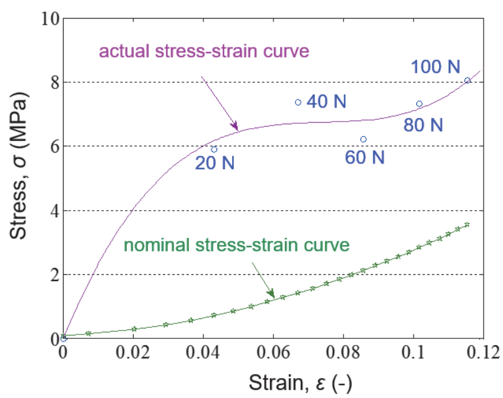

Figure 12: Compressive stress–strain curves of copy paper calculated by using the actual contact areas (red curve) and the nominal contact areas (green curve)

3.2 A more accurate method for calculating the stress–strain curve

As mentioned before, the carbon paper used for preliminary experiments was Geha-1. When the applied force is smaller than 20 N, this type of carbon paper is not sensitive enough to show the contact area. Figure 13 shows the force sensitivity of carbon paper Geha-1, for four different forces imposed on the surface of carbon paper. It can be seen that the contact area is not clear anymore when the force is smaller than 20 N. To improve the accuracy of the calculation results, some other tests should be implemented. It is better to find a much more sensitive material, to show the actual contact areas.

Seven other different types of carbon papers (SH-1, SH-2, SH-3, DL-1, DL-2, DL-3, Geha-2) from three different companies were selected. Two types of Fujifilm (Fuji-LLW and Fuji-LLLW) were also tested here. For each of the carbon papers, four different forces (2 N, 10 N, 20 N, and 100 N) were imposed on the materials.

It can be seen from Figure 14 that the sensitivities of different carbon papers are quite different; only SH-1, Geha-2 and Fuji-LLLW can be used for measuring low pressure. The sensitivity of SH-1 is very close to the sensitivity of Fuji-LLLW. When the force is smaller than 10 N, the contact areas can also be shown on the copy paper. The SH-1 carbon paper was selected in the following experiment for showing the contact areas under different forces.

The experimental process was reorganized as given in Section 2.2 and 50 groups of experiments were implemented. An example of contact area measurement is shown in Figure 15. The evaluation method was the same as before: all the pictures were transformed to the binary images and then the contact areas could be calculated. The calculated results are shown in Figure 16, where each point represents the average contact area of 20 tests under the same force.

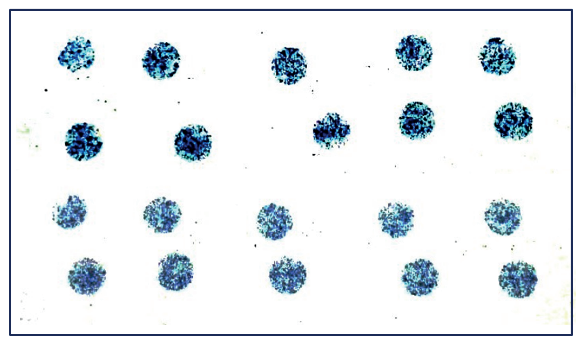

Figure 15: Example of measured contact areas (the force here is 90 N)

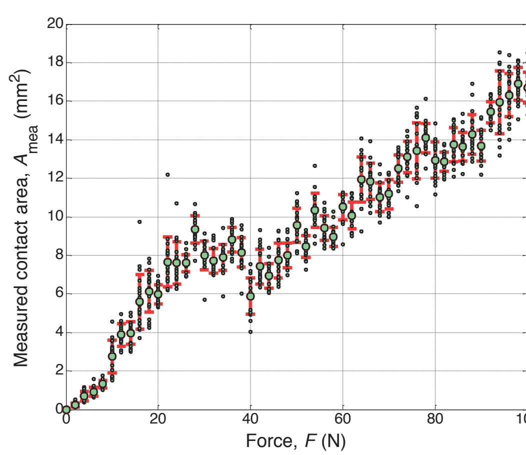

Figure 16: Measured contact areas for copy paper with SH-1 carbon paper under forces changed in steps of 2 N

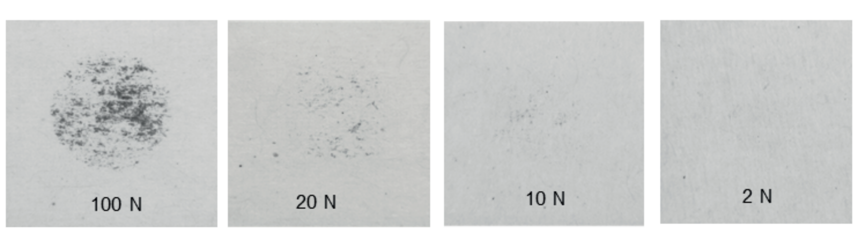

Figure 13: Sensitivity tests of carbon paper (Geha-1)

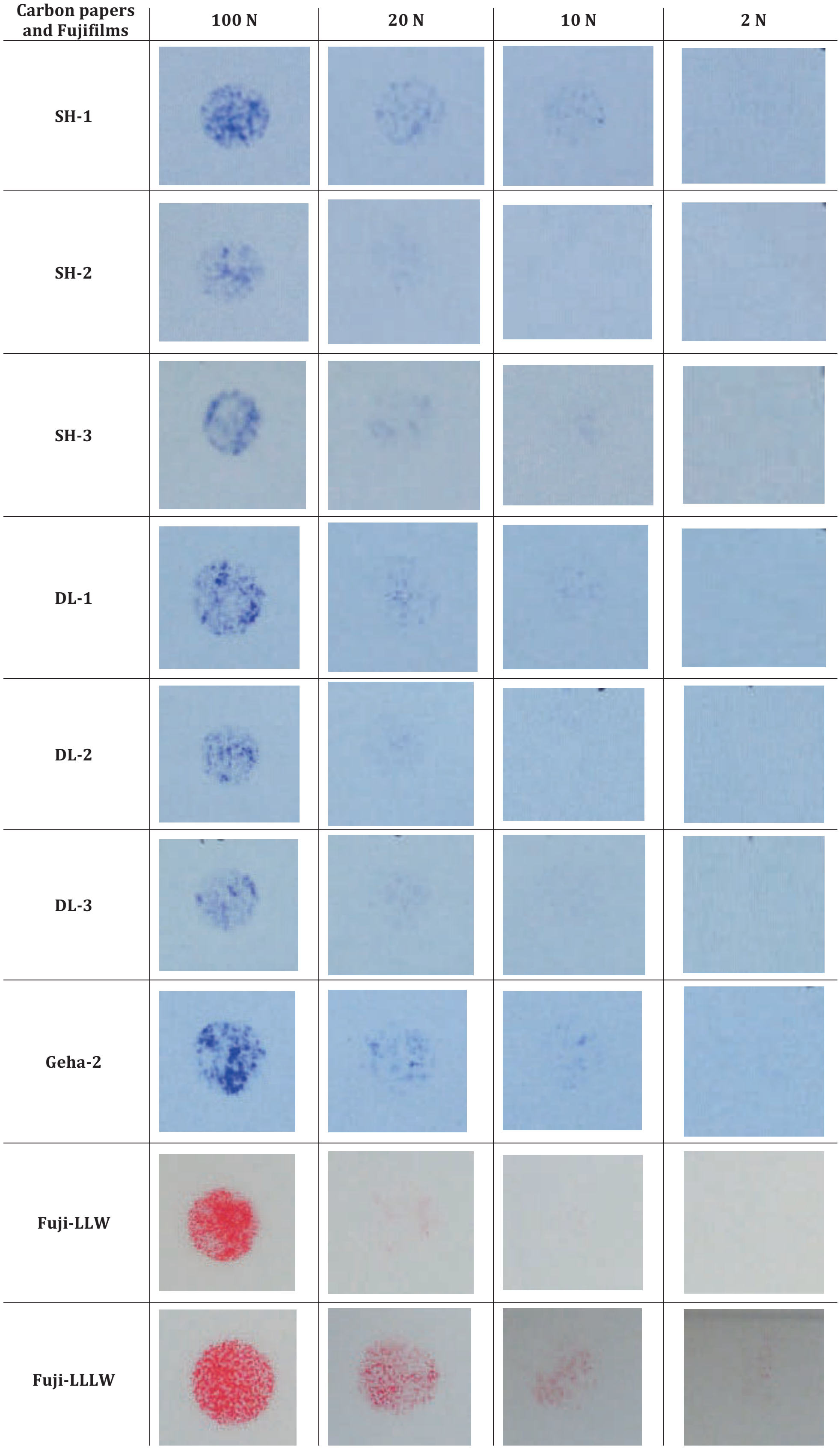

Figure 14: Sensitivity tests of seven different carbon papers and two Fuji-films

The average values of the measured contact areas under different forces were plotted in Figure 17 as discrete points. The relationship between the measured contact area A_{mea} and force F can be drawn by the curve fitting method. The cubic curve fitting method was used here; the fitting function is provided as follows:

$$A_{mea} = 3.6 \cdot 10^{-5} \cdot F^3 - 0.0057 \cdot F^2 + 0.39 \cdot F - 0.24 \qquad [8]$$

The calculation result (R^2 = 0.953) shows that this method can be well used to calculate the measured (actual) contact area A_{mea} ($A(z)$) under different forces $F(z)$.

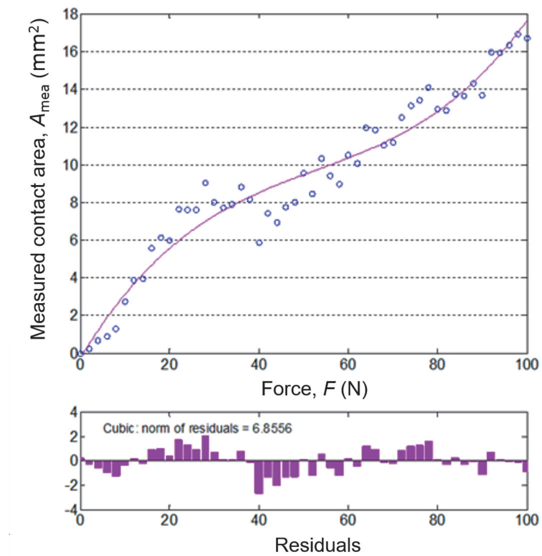

Figure 17: Measured contact areas for copy paper with SH-1 carbon paper under different forces with cubic curve fitting

By using this new method, we can redraw the actual modulus–strain curve (see Figure 18) and the actual stress–strain curve (see Figure 19).

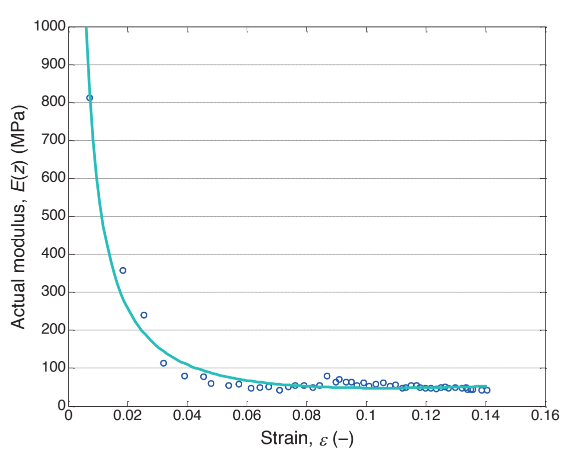

Figure 18: Relationship between the actual modulus and strain for copy paper with SH-1 carbon paper

Figure 18 shows the relationship between the actual modulus and the strain (or deformation). The discrete data were calculated according to Equation [3]. The blue curve is the corresponding curve fitting result (Equation [9]), R^2 = 0.977.

$$E(z) = -72.73 + 6730.15 \cdot z + 0.54 \cdot \frac{1}{z} \qquad [9]$$
$$z = 0.0847 \cdot \varepsilon$$

When the force is changed from 2 N to 100 N, the actual modulus of paper will decrease from 812 MPa to around 50 MPa. As mentioned before, at the beginning of the compression process, the actual modulus of paper is very big which is mainly because the actual contact area is very small. When the contact area approaches to the maximum contact area, the actual modulus will be decreased to a constant value.

According to Equations [4] and [8], the actual stress–strain curve of paper can also be recalculated. The new actual stress–strain curve is shown in Figure 19.

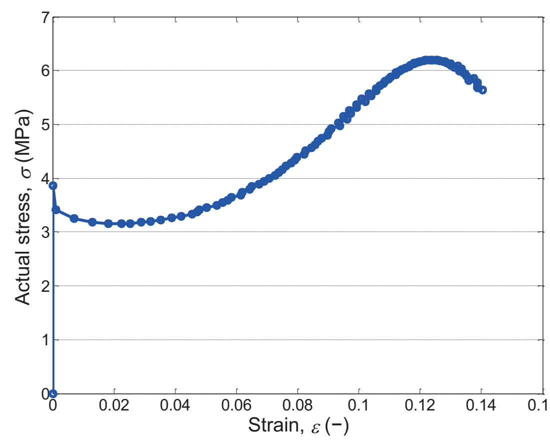

Figure 19: Compressive stress–strain curve of copy paper calculated by using the actual contact areas with SH-1 carbon paper

From Figure 19, we can reasonably infer that the surface topography has a considerable influence on the compressive behavior of paper materials.

When the surface roughness is taken into account, the stress–strain curve of paper material is not typically J-shaped anymore.

4. Discussion

Based on the results obtained in section 3, we can see that by considering the surface roughness, the stress–strain curve of paper material is more like that of a typical elastic-plastic material (see Figure 20). Many engineering materials show this kind of behavior, such as steels used for automotive seat structure (Yuce, et al., 2014), polymers with strain hardening behavior (Senden, 2013, p. 119), aluminum alloy and steel plates tested in laboratory (Liu, Villavicencio and Soares, 2013), and so on.

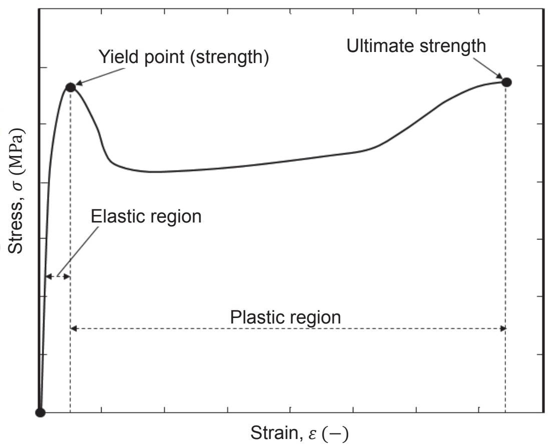

Figure 20: Typical stress–strain curve of an elastic-plastic material, adopted from Turner and Burr (1993)

As shown in Figure 20, some typical characteristics used for determining the elastic-plastic material, for example, the plastic region, the yield strength and the ultimate strength, etc., all of these behaviors can also be found in Figure 19.

The elastic region of paper material is relatively small, which means the behavior of paper material is more close to perfectly plastic materials.

Although, in most situations, the mechanical behavior of paper material is regarded as J-shaped. But it can be seen from the work done in this research that, in essence, paper is still an elastic-plastic material. The surface roughness plays a very important role in presenting the mechanical behavior.

In addition, for the compression behavior of paper material, the obtained stress–strain curve after ultimate stress is decreasing, rather than increasing, which may be caused by the change of the internal structure or by the selected curve fitting function (see Figure 17).

5. Conclusions

First of all, two important concepts were presented in this paper: the actual compression modulus and the actual stress–strain curve of paper. Paper is not a linearly elastic material. The elastic modulus (*E*-modulus) of a material with non-linear elastic stress–strain response was defined as the slope of the tangent line to the stress–strain curve at the origin and therefore depends only on the small strain behavior. Because of the long experience with linearly elastic metals, the idea of an *E*-modulus was carried over to paper, but the physical meaning of such a modulus for paper is not clear (Mark, et al., 2001). In this paper, the concept of actual modulus is presented. The actual compression modulus of paper is not a constant value, which was also calculated. Then, nearly all research works presented up to now discussed the stress–strain curve of paper by using the nominal contact area. But actually, the stress–strain curve of paper is apparently affected by the surface topography. So the concept of actual stress–strain curve was introduced here to study the mechanical behavior of paper materials.

In addition, a new experimental method was proposed to calculate the actual contact areas. Its calculation results identified the practicability of the method. Different types of carbon papers have been selected and compared. With the help of actual contact areas obtained, the actual compression modulus and the actual stress–strain curve of copy paper were calculated. The calculation results show the crucial differences between the actual and nominal stress–strain behaviors.

In summary, according to the presented research results, the stress–strain curve of paper calculated by using the actual contact area is totally different from the calculation result of the nominal contact area. The mechanical behavior of paper materials under compressing by considering the surface roughness is very close to the general elastic-plastic materials. The influence of the surface roughness cannot be ignored and special attention should be given to the research of the paper surface topography.

Acknowledgements

The authors gratefully acknowledge the financial support from the Jiangsu Science and Technology Department (Project Number: BK20190873). All experiments mentioned in this paper were implemented by using the testing machine ZWICK Z050 in IDD (Institute of Printing Science and Technology, Technische Universität Darmstadt).

List of Abbreviations

A_0	Nominal contact area
A_{ind}	Nominal area of the indenter, which is equal to the value of the nominal contact area A_0
A_{mea}	Measured contact area, which is regarded as equivalent to the actual contact area $A(z)$
$A(z)$	Actual contact area, which is changing with deformation z
d	Original thickness of the paper (d = 0.0847 mm)
E	E-modulus, which is a constant value
$E(z)$	Actual modulus, which is changing with deformation
F	Force
$F(z)$	Force when the deformation is z
l_0	Original length or thickness of the material
R_a	Average profile roughness
S_a	Average areal roughness
S_{ind}	Average areal roughness of the indenter
S_{pla}	Average areal roughness of the platform
$W(z)$	Actual contact pressure
z	Deformation of paper in the out-of-plane direction
ε	Strain
σ	Stress

References

Alam, A., Thim, J., Manuiskiy, A., O'Nils, M., Westerlind, C., Lindgren, J. and Lidén, J., 2011. Investigation of the surface topographical differences between the Cross Direction and the Machine Direction for newspaper and paperboard. *Nordic Pulp & Paper Research Journal*, 26(4), pp. 468–475. https://doi.org/10.3183/npprj-2011-26-04-p468-475.

Bachus, K.N., DeMarco, A.L., Judd, K.T., Horwitz, D.S. and Brodke, D.S., 2006. Measuring contact area, force, and pressure for bioengineering applications: using Fuji Film and TekScan systems. *Medical Engineering & Physics*, 28(5), pp. 483–488. https://doi.org/10.1016/j.medengphy.2005.07.022.

Buchner, B., 2008. *Investigation of friction in closed-die warm forging of aluminium alloys*. Doctoral thesis. University of Leoben.

Chen, L., Ahadi, A., Zhou, J. and Ståhl, J., 2013. Modeling effect of surface roughness on nanoindentation tests. *Procedia CIRP*, 8, pp. 334–339. https://doi.org/10.1016/j.procir.2013.06.112.

Chen, L., Ahadi, A., Zhou, J. and Ståhl, J., 2014. Numerical and experimental study of the roughness effects on mechanical properties of AISI316L by nanoindentation. *Modeling and Numerical Simulation of Material Science*, 4(4), pp. 153–162. http://dx.doi.org/10.4236/mnsms.2014.44017.

Deutsche Institut für Normung, 1993. *DIN EN 20187:1993-11 Papier, Pappe und Zellstoff; Normalklima für die Vorbehandlung und Prüfung und Verfahren zur Überwachung des Klimas und der Probenvorbehandlung (ISO 187:1990); Deutsche Fassung EN 20187:1993*. Berlin: DIN.

Deutsche Institut für Normung, 2018. *DIN 50014:2018-04 Normalklimate für Vorbehandlung und/oder Prüfung – Festlegungen*. Berlin: DIN.

Drexler, E., 2009. Nanostructures, nanomaterials, and lattice-scalled stiffness. *Metamodern: the trajectory of technology*, [blog] 15 February. Available at: <http://metamodern.com/2009/02/15/nanomaterials-nanostructures-and-stiffness/> [Accessed March 2020].

Endres, I., 2006. *Compression uniformity measurements on coated and uncoated paper surfaces*. Doctoral thesis. University of Karlstad.

Fujifilm, 2016. *Prescale Sheet Type*. [online] Fujifilm Corporation. Available at: <https://www.fujifilm.com/products/prescale/prescale_sheettype/> [Accessed March 2020].

Hansson, P. and Johansson, P.-Å., 2000. Topography and reflectance analysis of paper surfaces using a photometric stereo method. *Optical Engineering*, 39(9), pp. 2555–2561. https://doi.org/10.1117/1.1287261.

Kaulitz, T., 2009. *Bilden von Schneidlagen unter Ausnutzung des Nipinduzierten Effekts für die Druckweiterverarbeitung*. Doctoral dissertation. Technische Universität Darmstadt.

Kaulitz, T. and Dörsam, E., 2008. Highly accurate material characterization of paper for the simulation of printing process. In: N. Enlund and M. Lovreček, eds. *Advances in Printing and Media Technology: Proceeding of the 35th International Research Conference of iarigai*. Valencia, Spain, September 2008. Darmstadt, Germany, pp. 263–270.

Liu, B., Villavicencio, R. and Soares, C.G., 2013. Failure characteristics of strength-equivalent aluminium and steel plates in impact conditions. In: C. Guedes Soares and J. Romanoff, eds. *Analysis and Design of Marine Structures: Proceedings of the 4th International Conference on Marine Structures (MARSTRUCT 2013).* Espoo, Finland, 25–27 March 2013. Boca Raton, FL, USA: CRC Press, pp. 167–174.

Luong, C.H., 1999. *Experimental and theoretical investigations of mechanical and thermal relations by calendering of paper*. Doctoral thesis. Norwegian University of Science and Technology, Trondheim.

Mark, R.E., Haberger Jr., C.C., Borch, J. and Lyne, M.B. eds., 2001. *Handbook of physical testing of paper: Volume 1.* 2nd ed. Boca Raton, FL, USA: CRC Press.

MATLAB Help, 2013. *Image processing toolbox: user's guide – R2013b.* [pdf] MathWorks. Available at: <http://www.mathworks.com/downloads> [Accessed March 2020].

Otsu, N., 1979. A threshold selection method from gray-level histograms. *IEEE Transactions on Systems, Man and Cybernetics*, 9(1), pp. 62–66. https://doi.org/10.1109/TSMC.1979.4310076.

Pino, A. and Pladellorens, J., 2009. Measure of roughness of paper using speckle. In: P.S. Huang, T. Yoshizawa and K.G. Harding, eds. *Proceedings Vol. 7432: SPIE optical Engineering + Applications.* San Diego, CA, USA, 2–6 August 2009. SPIE, pp. 74320. https://doi.org/10.1117/12.825072.

Provatas, N. and Uesaka, T., 2003. Modelling paper structure and paper-press interactions, *Journal of Pulp and Paper Science*, 29(10), pp. 332–340.

Rättö, P., 2005. The influence of surface roughness on the compressive behaviour of paper, *Nordic Pulp and Paper Research Journal*, 20(3), pp. 304–307. https://doi.org/10.3183/npprj-2005-20-03-p304-307.

Schaffrath, H.-J. and Göttsching, L., 1991. The behavior of paper under compression in z-direction. In: *Proceedings of the 1991 Tappi International Paper Physics Conference.* Kona, HI, USA, 22–28 September 1991. Atlanta, USA: TAPPI Press, pp. 489–510.

Schaffrath, H.-J. and Göttsching, L., 1992a. Das Kompressionsverhalten von Papier in ZD. *Das Papier*, 46, pp. 74–81.

Schaffrath, H.-J. and Göttsching, L., 1992b. Modellierung der Kompression von Papier in z-Richtung bei niedriger Flächenpressung. *Das Papier*, 46(7), pp. 350–355.

Senden, D.J.A., 2013. *Strain hardening and anisotropy in solid polymers*. Doctoral thesis. Technische Universiteit Eindhoven.

Singh, S.P., 2008. A comparison of different methods of paper surface smoothness evaluation. *BioResources,* 3(2), pp. 503–516.

Stenberg, N., 2003. A model for the through-thickness elastic-plastic behaviour of paper. *International Journal of Solids and Structures,* 40(26), pp. 7483–7498. https://doi.org/10.1016/j.ijsolstr.2003.09.003.

Teleman, A., Östlund, C., Nordström, J.-E., Johansson, P.-Å. and Vomhoff, H., 2004. *Analysis of paper surface topography under compression: STFI report CW217*. Stockholm, Sweden: STFI.

Turner, C.H. and Burr, D.B., 1993. Basic biomechanical measurements of bone: a tutorial. *Bone*, 14(4), pp. 595–608. https://doi.org/10.1016/8756-3282(93)90081-K.

Vernhes, P., Bloch, J.-F., Blayo, A. and Pineaux, B., 2009. Effect of calendering on paper surface micro-structure: a multi-scale analysis. *Journal of Materials Processing Technology*, 209(11), pp. 5204–5210. https://doi.org/10.1016/j.jmatprotec.2009.03.005.

Vernhes, P., Dubé, M. and Bloch, J.-F., 2010. Effect of calendering on paper surface properties. *Applied Surface Science*, 256(22), pp. 6923–6927. https://doi.org/10.1016/j.apsusc.2010.05.004.

Xia, Q.S., Boyce, M.C. and Parks, D.M., 2002. A constitutive model for the anisotropic elastic-plastic deformation of paper and paperboard. *International Journal of Solids and Structures,* 39(15), pp. 4053–4071. https://doi.org/10.1016/S0020-7683(02)00238-X.

Yuce, C., Karpat, F., Yavuz, N. and Sendeniz, G., 2014. A Case study: designing for sustainability and reliability in an automotive seat structure. *Sustainability*, 6(7), pp. 4608–4631. https://doi.org/10.3390/su6074608.

JPMTR 130 | 1914
DOI 10.14622/JPMTR-1914
UDC 651.5:546.57|7.048

Research paper
Received: 2019-12-25
Accepted: 2020-03-26

Optimisation of aerosol jet deposition for high-resolution selective patterning of silver tracks

Ben Clifford, Chris Phillips and Davide Deganello

Welsh Centre for Printing and Coating,
College of Engineering, Swansea University,
Fabian Way, Swansea, SA1 8EN, UK

b.r.clifford@swansea.ac.uk
c.o.phillips@swansea.ac.uk
d.deganello@swansea.ac.uk

Abstract

Aerosol jet deposition is a digital direct-write additive manufacturing technique capable of producing high resolution and highly customisable electronic and biological functional devices on both two- and three-dimensional substrates. This technology offers important market opportunities in the production of consumer electronics, semiconductor packaging, display technology, aerospace and defence, automotive and life sciences. However, for these opportunities to be realised there is a necessity for greater understanding of how deposition process parameters influence deposition quality. This study has explored the effects of a number of these parameters and their influence on the geometry of printed features. The results of this work outline the operating windows for several deposition parameters including carrier gas flow rate, stage speed working distance and stage temperature. Additionally, a number of relationships have been identified linking deposition parameters to the geometry of printed features.

Keywords: printed electronics, high-resolution printing, metal printing, parameter optimisation, surface topography

1. Introduction and background

Aerosol jet deposition is a direct-write non-contact deposition process originally developed for the manufacture of electronic circuits and printing of electronic materials. Since then its use as a deposition technology for a wide range of functional materials including metals, polymers and even biologicals has emerged (Zöllmer, et al., 2006). The compatibility of the technique with such a wide range of materials has seen the development of an assortment of novel applications in key research areas including printed electronics and sensors (Zhao, et al., 2012; Clifford, et al., 2018; Cantù, et al., 2018), renewable energy (Mette, et al., 2007) and biological/biomedical devices (Marquez, Renn and Miller, 2001).

Whilst the number of publications relating to aerosol jet deposition is increasing year on year, the majority of these are focussed on new applications of the technology and there is a lack of published research and understanding relating to the science and theory behind the process. This limited understanding in the field has resulted in recent publications reitterating the statement made over a decade ago that full and accurate process modelling and optimisation is required (Wilkinson, et al., 2019; Hon, Li and Hutchings, 2008; Zhang, Liu and Whalley, 2009).

The aerosol jet deposition process works by atomising, either ultrasonically or pneumatically, a solution or suspension containing a functional material suited to the desired application. Micron sized droplets become separated from the bulk material and become entrained in a carrier gas stream which transports them to a deposition head. This droplet loaded gas stream is then aerodynamically focussed by a secondary gas stream, referred to as the sheath gas, through a converging nozzle forming a collimated beam. The substrate is positioned several millimetres below the nozzle on a motion controlled heated stage, and patterning is achieved by the relative movement of the substrate and deposition head (Clifford, et al., 2018; Hoey, et al., 2012). A photograph of the aerosol jet deposition system at Swansea University with an illustrative diagram of the aerosol jet process is shown in Figure 1 (Clifford, 2017).

Process optimisation is complex with a large number of both primary and secondary parameters which can be varied to change the resolution and profile of depositions. On top of this, getting qualitative data from

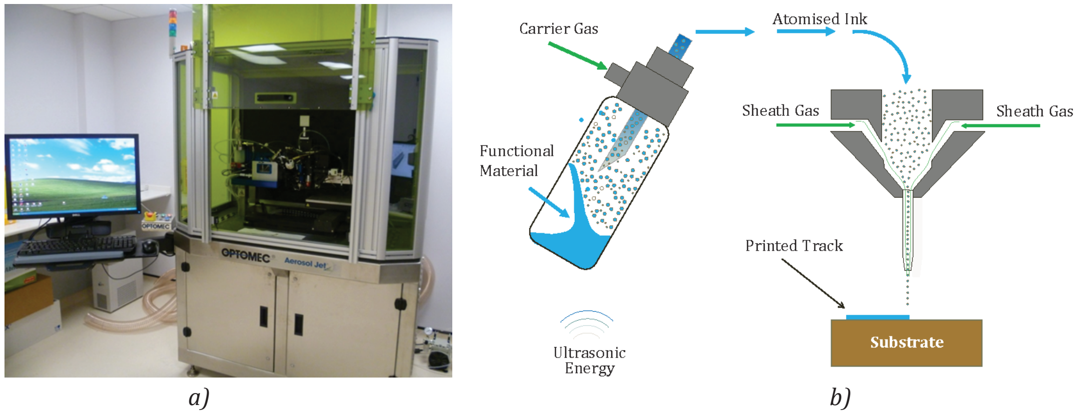

Figure 1: (a) Photograph of the AJ300 aerosol jet deposition system at Swansea University; (b) an illustrative diagram showing the ultrasonic atomisation and aerosol jet deposition process

optical measurements of unoptimised prints is often complicated by poorly defined edges and unwanted deposition phenomena including overspray and satellite droplets.

In 2011, Goth, Putzo and Franke described the main influencers affecting aerosol jet deposition quality, grouping them into six categories: robot, process control, operator, ink, substrate and environment, each containing a set of individual parameters. An adapted Ishikawa diagram based on the work presented by Goth, Putzo and Franke (2011) is shown in Figure 2 highlighting these categories.

Whilst there are several research papers looking at parametric studies of the aerosol jet system, the majority of the work is directed to exploring the influence of the ratio of the carrier gas and sheath gas flow rates (Mahajan, Frisbie and Francis, 2013; Arsenov, Efimov and Ivanov, 2018). In this paper, we present a study of the effects of several additional process parameters, namely, atomiser (or carrier) gas flow rate; working (nozzle-substrate) distance; stage speed and stage temperature, on the geometry of printed silver lines.

The findings of this work can be used to identify the operating window of individual parameters as well to outline those that are critical to achieving high-resolution features as well as secondary and complementary parameters.

2. Materials and methods

2.1 Ink

All printing during the process study was carried out using a commercial nanoparticle silver ink TPS 35 HE (Clariant Produkte (Deutschland) GmbH). This ink is designed to be used for inkjet printing and is quoted as having a dynamic viscosity of 6.5 mPas at 20 °C and a surface tension of 28.2 mN/m. The solids loading of this ink is approximately a mass fraction of 35 % with an average particle size of approximately 60 nm. The solvent in which the particles are dispersed is a blend of water and ethylene glycol. In order to make this ink compatible with the ultrasonic atomiser of the aerosol jet system, it was diluted with distilled water at a ratio of 1:2 parts by volume.

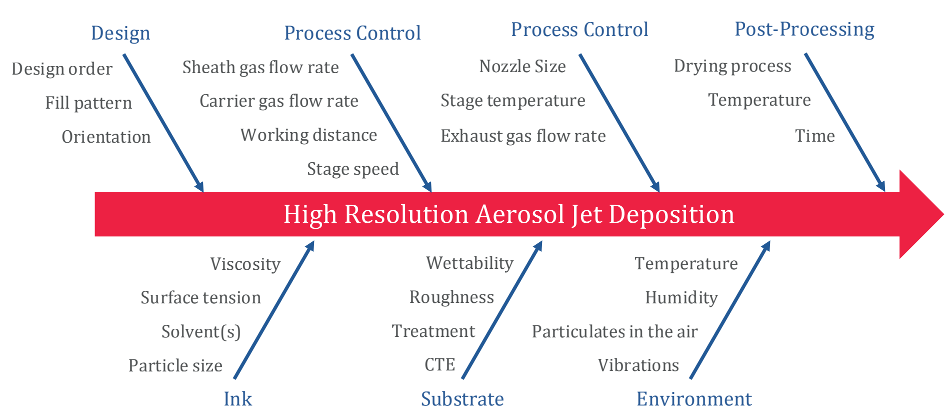

Figure 2: An Ishikawa diagram showing the large parameter set affecting aerosol jet deposition feature geometry and resolution

2.2 Substrate

Standard glass microscope slides (12383118, Fisher Scientific) of length and width of 76 mm and 26 mm with a thickness between 1 and 1.2 mm were used as the test substrate. Glass microscope slides were chosen for their low roughness, transparency and consistency between batches. The low roughness provided a clean base for surface topology and profile measurements whilst the transparency allowed backlit illumination to be used in the detection of overspray. The average surface roughness, S_a, and the root mean square (RMS) surface roughness, S_q, of these microscope slides was measured using white light interferometry to be 9.18 nm and 12.73 nm, respectively.

Prior to deposition, the glass slides were prepared by ultrasonic cleaning in acetone, propan-2-ol and deionised water for 10 minutes in each. Following the cleaning process the glass slides were dried and placed on a hot plate at 200 °C for 30 minutes before they were transferred to the system for printing. The deposited ink showed good levels of wetting with the cleaned glass slides and hence no additional surface pre-treatment/modification was required.

2.3 Printing methodology

Deposition was performed with an AJ300 aerosol jet deposition system (Optomec Inc., Albuquerque, USA) using an ultrasonic atomiser operating at 2.4 MHz. For all experiments a number of parameters including the nozzle, atomiser power and ink temperature were kept constant. The nozzle used had a 200 µm diameter opening with a taper half angle of a few degrees. The atomiser power was set to ≈ 31 W by applying a voltage of 48 V and a current of ≈ 650 mA. For each print run, the atomiser vial was loaded with 1.80 ml of the diluted ink described in section 2.1 and maintained at 20 °C by means of a temperature-controlled water bath.

Two designs were selected as test patterns to allow geometric characterisation in terms of line width and height whilst providing the ability to identify the effects of varying these parameters on overspray and satellite deposition. The first toolpath consisted of six parallel horizontal lines each positioned 1 mm apart; three lines of 10 mm in length and three lines of 20 mm in length to allow testing at high (≥ 10 mm/sec) process velocities whilst ignoring any initial acceleration. The second design was a smaller serpentine pattern of length 5 mm and pitch of 0.5 mm used to create prints which could be optically imaged in a single scan.

Following deposition, samples were dried in a natural convection oven (UNB400, Memmert GmbH) at 200 °C for 60 minutes and stored in sealed Petri dishes prior to measurement and analysis.

Prior to performing the experiments described, a literature survey and initial screening trial was performed to identify suitable parameters and the operating ranges for each. This revealed a number of parameters that have a significant impact on deposition quality. The work presented here shows the results of adjusting these key parameters and full results including secondary parameters can be seen in the thesis titled “Optimisation of Aerosol Jet Deposition for the Development of Printed Electronics” (Clifford, 2017).

The parameters studied in this work are shown in Table 1 along with the ranges used for testing. For each parameter investigated three prints were produced, with 30 measurements made across each sample (5 equidistant points on each line) giving a total of 150 data points per variation.

The carrier gas flow rate determines the quantity of atomised material that is transferred to the deposition head and one of two parameters affecting the volume of material deposited in one location on the substrate. The stage speed is the second of these parameters and controls the process velocity of the stage, and substrate, relative to the deposition head. The carrier gas flow rate and stage speed have a positive relationship meaning as the atomiser flow rate is increased the stage speed must also be increased to produce the same geometry features. As material exits the nozzle as a highly collimated stream the sheath gas immediately begins to diverge giving the stream a limited

Table 1: The parameters tested with a brief description of what they affect with the range of values that were tested

Parameter	Description	Range Tested
Carrier Gas Flow Rate	Controls the quantity of material delivered to the deposition head.	12–24 cm^3/min
Stage Speed	The speed the stage (and substrate) moves relative to the fixed deposition head and nozzle.	1–10 mm/sec
Nozzle–Substrate Distance	The distance material travels between exiting the nozzle and impacting with the substrate.	2–11 mm
Stage Temperature	The temperature of the stage that the substrate is positioned on during printing.	25–100 °C

focussing length. The distance between the nozzle exit and the substrate whereby the material stream needs to remain focussed is termed the nozzle–substrate distance. The stage temperature affects the drying rate of the deposited material and as such the final geometry of printed features.

2.4 Surface topography measurement

Optical images of deposited features were gathered using an Alicona G5 infinite focus microscope (Alicona Imaging GmbH, Austria) in order to visually explore deposition quality. As well as visualisation of the deposits, this provided a method to qualitatively assess the deposited features in terms of unwanted attributes such as overspray and satellite deposition.

White light interferometry (NT9300, Veeco Instruments Inc., Plainview, NY, USA) was used to obtain surface topography data for each printed line. Measurements were collected at eleven times magnification (achieved using a twenty times magnification lens with a 0.55 times field of view modifier), giving a measurement area of 0.58 mm by 0.43 mm at a resolution of 640 × 480 pixels. For each print, the geometry was measured at ten discrete points along the length of the line. Measurements were taken of the line width and average height (taken as the average height of the substrate subtracted from the average height of the ink) as well as reviewing the profile shape.

3. Results and discussion

3.1 Carrier gas

The carrier gas flow rate is one of two primary parameters affecting the volume of material deposited in one location – the other being the stage speed. In order to investigate the effect of the carrier gas flow rate on the geometry of printed features, deposition was performed at a range of carrier gas flow rates between 12 cm^3/min and 24 cm^3/min whilst maintaining a constant sheath gas flow rate of 90 cm^3/min. Additionally, the stage speed was maintained at a constant value of 1 mm/s with a stage temperature of 100 °C.

The measured line width and average line height data is plotted graphically in Figures 3a and 3b separately.

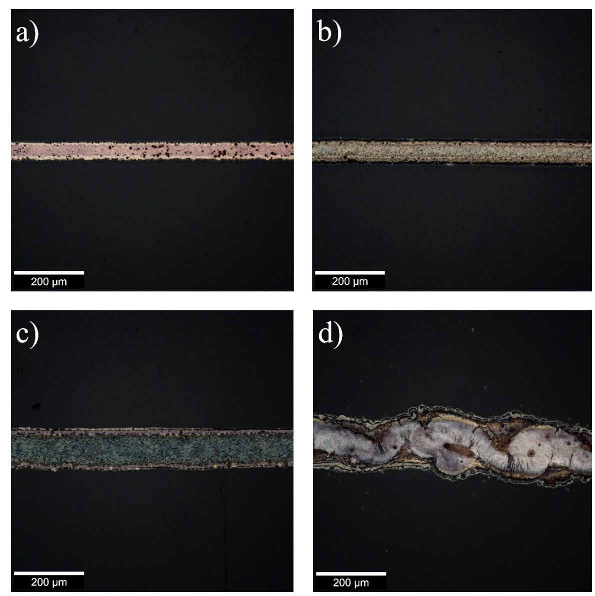

Figure 4: Optical microscope images showing the effect of carrier gas flow rate of (a) 12 cm^3/min, (b) 16 cm^3/min, (c) 20 cm^3/min, and (d) 24 cm^3/min on deposited line geometry using a constant sheath gas flow rate of 90 cm^3/min; scale bar for reference is 200 µm

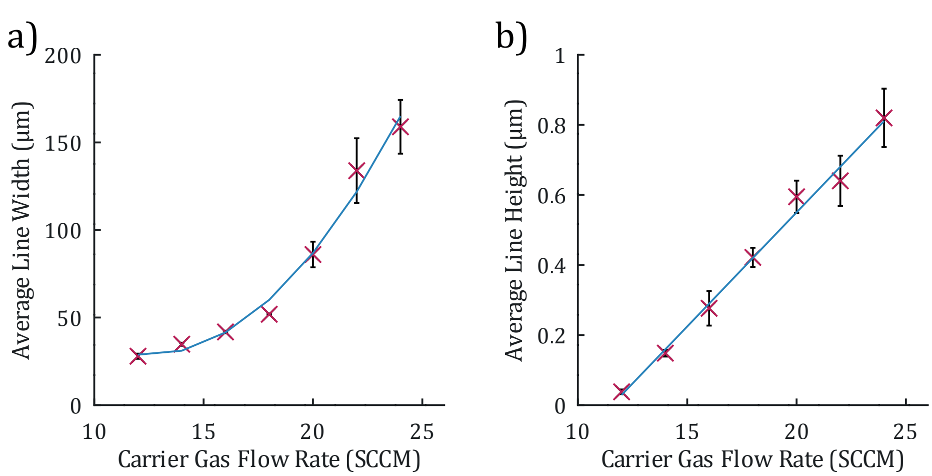

Figure 3: Graphs showing the effect of carrier gas flow rate on (a) average line width, and (b) average line height

The data shows that as the carrier gas flow rate increases both the width and height of deposited line also increases. Initially, for carrier gas flow rates between 12 cm^3/min and 18 cm^3/min the line width shows a linear trend with low standard deviations but as the flow rate increases further the line width and standard deviation increase rapidly diverging from the trend. This sudden increase is linked to the stage speed being too low allowing large quantities of material to build up in one location. This can be seen visually in the optical microscope images shown in Figures 4a to 4d taken of lines deposited at carrier gas flow rates of 12 cm^3/min, 16 cm^3/min, 20 cm^3/min and 24 cm^3/min, respectively.

3.2 Stage speed

The stage speed is the second parameter affecting the volume of material deposited in one location. In order to investigate the effect of stage speed on the geometry of printed features (Figure 5), deposition was performed at stage speeds between 1 mm/s and 10 mm/s. During the experiment, the sheath and carrier gas flow rates were kept constant at 112 cm^3/min and 16 cm^3/min, respectively. The stage temperature was maintained at a constant value of 100 °C.

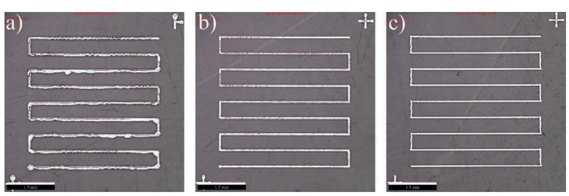

Figure 5: Optical microscope images showing the effect of stage speed on deposited line geometry; stage speed of (a) 1 mm/s, (b) 4 mm/s, and (c) 10 mm/s; scale bar for reference is 1.5 mm

The average line width and line height data are plotted graphically in Figures 6a and 6b separately. From these graphs it can be seen that as the stage speed increases there is a decrease in both line width and line height as less material is deposited in each area. The line width and height decrease steadily as stage speed increases from 1 mm/s to 3 mm/s. After this point, the sensitivity of the deposit to stage speed is reduced. The rate of decrease in line width and height is higher at low speed transitions due to the larger printed length for the given carrier gas flow rate. As an example, with the sheath and carrier gas flow rates described previously, an increase in stage speed from 1 mm/s to 2 mm/s causes a decrease in line width of 11.22 µm. In contrast at the same flow rates, an increase in stage speed from 6 mm/s to 7 mm/s causes a much smaller drop in line width – 1.29 µm. This highlights the relationship between the carrier gas flow rate and the stage speed previously discussed.

3.3 Nozzle–substrate distance

As a result of the nozzle profile and annular sheath gas flow, the material exits the nozzle as a highly collimated converging beam which becomes finest at a focal point before rapidly diverging. In order to investigate the effect of the nozzle-substrate distance on the geometry of printed features, deposition was performed with the nozzle positioned between 2 mm and 11 mm above the substrate. During the experiment, both the carrier and sheath gas flow rates were kept constant at 20 cm^3/min and 100 cm^3/min, respectively. The stage speed was set to 2 mm/s with the temperature at 100 °C.

At each working distance, measurements of line width and height were taken using white light interferometry as well as imaged using optical microscopy. For each printed line multiple measurements were performed using white light interferometry, and the results are presented graphically in Figure 7. Due to the poor quality and large amounts of overspray and satellite deposition seen in the lines deposited at working distances greater than 9 mm it was not possible to obtain line width and line height measurements.

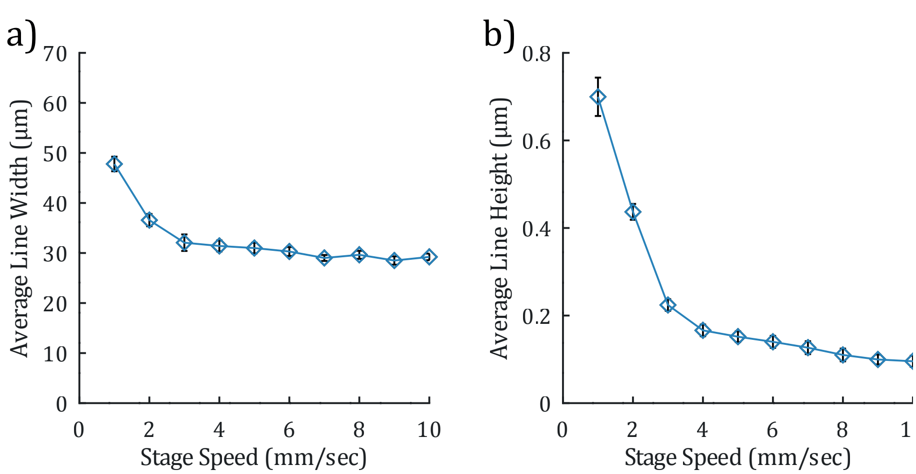

Figure 6: Graphs showing the effect of stage speed on (a) average line width, and (b) average line height

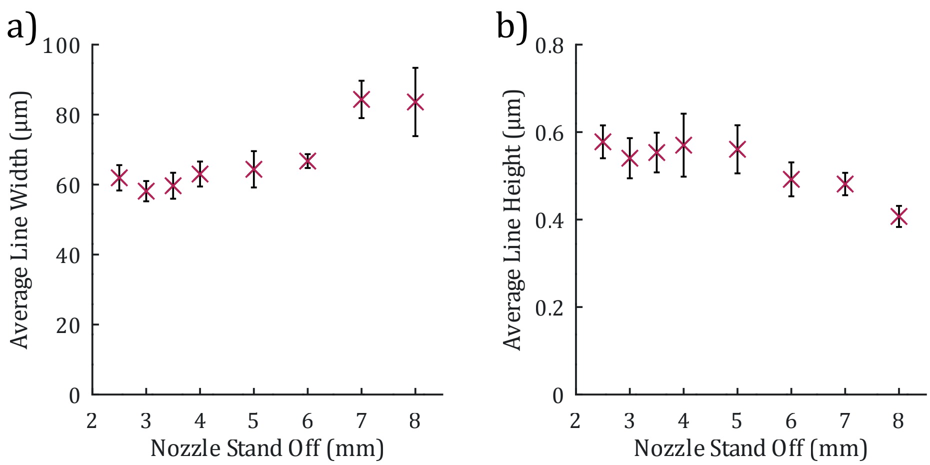

Figure 7: Graphs showing the effect of nozzle–substrate distance on (a) average line width, and (b) average line height

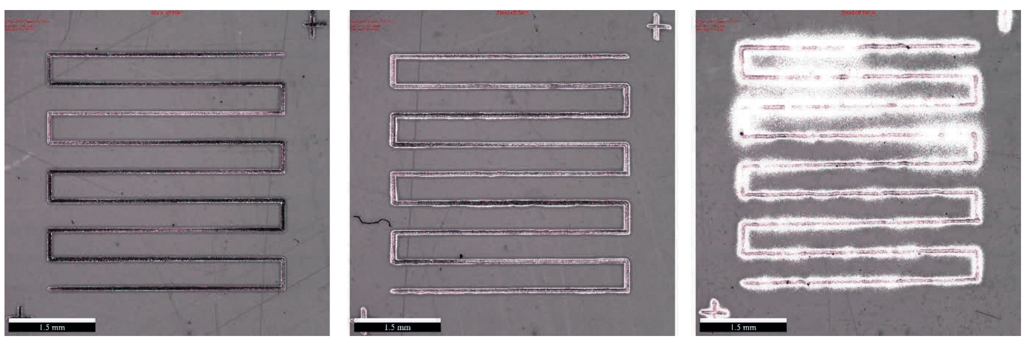

a) b) c)

Figure 8: Optical microscope images showing the effect of nozzle–substrate distance on deposited line geometry; on deposited line with a nozzle–substrate distance of (a) 3 mm, (b) 7 mm, and (c) 11 mm; scale bar for reference is 1.5 mm

Figure 8 shows microscope images of a low-density serpentine pattern deposited at nozzle–substrate distances of 3 mm (Figure 8a), 7 mm (Figure 8b) and 11 mm (Figure 8c). The line deposited at a working distance of 3 mm has well defined edges with no visible overspray, the line deposited at a working distance of 7 mm has some observable waviness at the edges with small amounts of overspray. In contrast the line deposited at a working distance of 11 mm has poorly-defined edges with large amounts of overspray obscuring the printed pattern.

3.4 Stage temperature

During deposition the substrate is positioned on a heated stage to aid in the drying of the ink. In order to investigate this parameter, the carrier and sheath gas flow rates were kept constant at 18 cm^3/min and 72 cm^3/min respectively with the stage speed set to 3 mm/s. The stage temperature was varied between 25 °C and 100 °C in increments of 25 °C with the purpose of investigating its effect on the deposited line geometry.

For each printed line multiple measurements were performed using white light interferometry and the results are presented graphically in Figure 9.

Figure 9 shows the effect of increasing stage temperature on line geometry. For stage temperatures below 100 °C, as the temperature increases the width of line also increases. In contrast, at a stage temperature of 100 °C a decrease in the line width is observed.

Additionally, as the stage temperature increases the standard deviation in the average line width decreases from 1.99 µm at 25 °C to 1.32 µm at 100 °C. Since the ink contains a volume fraction of approximately 84 % water which has a boiling point of around 100 °C, a large percentage of the water content is readily evaporated upon impact with the substrate. This could explain the decreased average line width at a stage temperature of 100 °C but further investigation is required involving inks containing different boiling point solvents. This explanation is also supported by examining the profiles of deposited lines at each stage temperature as shown in Figure 10.

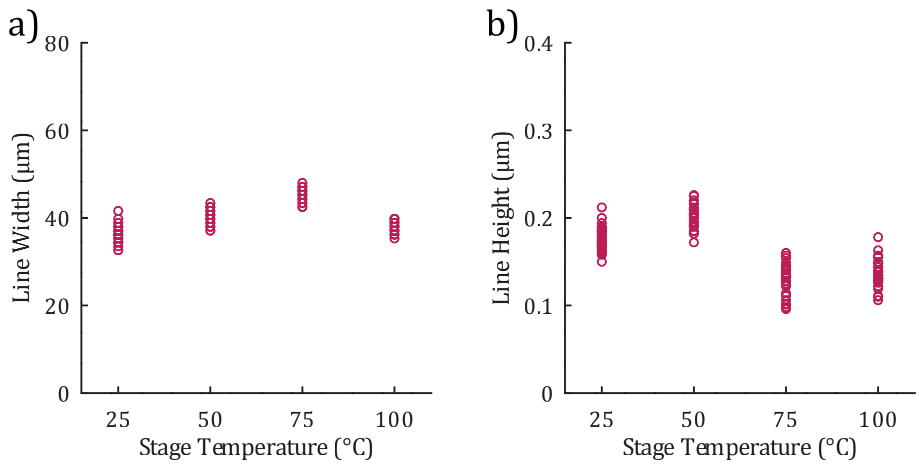

Figure 9: Graphs showing the effect of stage temperature on (a) average line width, and (b) average line height

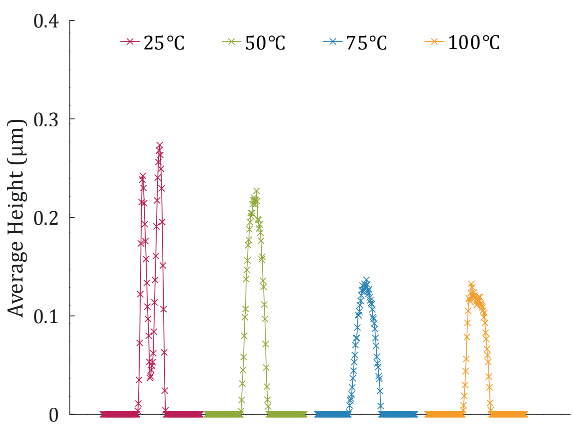

Figure 10: A graph showing the effect of stage temperature on the profile shape of deposited lines

By studying the visualisation in Figure 10, significant differences can be seen between the line profiles as a result of different stage temperatures.

At 25 °C the profile shows two distinct peaks with a central void often described in printing terminology as coffee-stain effect. As the stage temperature increases the height of the line profile reduces and the profile becomes more rectangular at 100 °C.

3.5 Deposition quality achieved with the optimised parameters

The optimisation of the parameters discussed has allowed for deposition of high resolution printed features as shown in Figures 11 and 12.

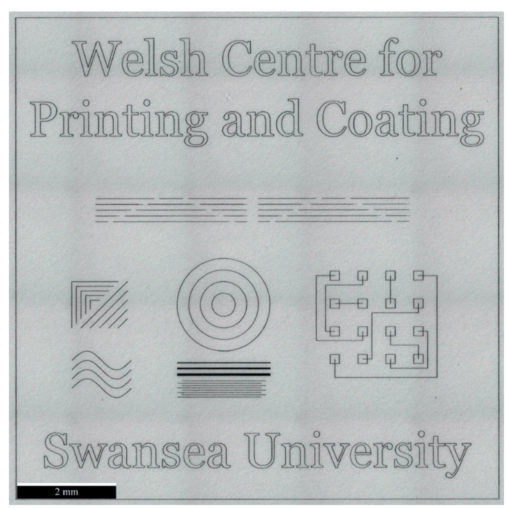

Figure 11: A microscope image showing a test pattern printed using aerosol jet deposition; scale bar for reference is 2 mm

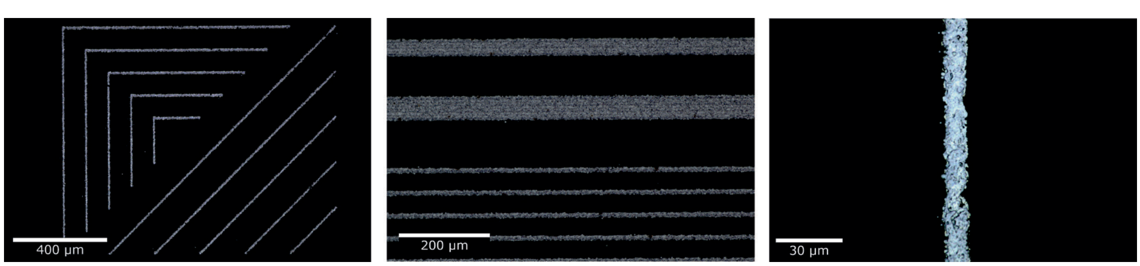

a) b) c)

Figure 12: Microscope images showing close up images of the features in Figure 11; scale bars are on (a) 400 µm, (b) 200 µm, and, (c) 30 µm, respectively (note: The contrast of this image has been adjusted in GIMP 2.10.14)

The deposited features have an average line width of around 10 µm with low amounts of overspray and satellite deposition with other lines shown with line widths of 30 µm, 40 µm and 50 µm.

4. Conclusions

From this study, the stage temperature and nozzle–substrate distance have been identified as critical parameters to obtaining high resolution defect free deposition. The stage temperature has been shown to have a significant effect on the geometry and resolution of printed features which has been theorised to be as a result of the formulation of the ink being tested. A relationship has been identified between the nozzle–substrate distance and unwanted deposition phenomena such as overspray and satellite droplets affecting overall resolution.

The effects of varying the carrier gas flow rate and stage speed have been shown to be linked to one another and whilst they do affect the geometry of deposited features, they do not directly affect resolution within their normal operating ranges. It is also possible to adjust these parameters in parallel to allow for thicker deposits with larger volumes of material or to maintain thinner deposits but reduce overall print time.

Whilst a significant number of parameters have been evaluated in this work, there are still parameters which have not been reviewed as well as other relationships that may be exist with relation to print design and material formulation.

Acknowledgements

This work was financially supported by the College of Engineering at Swansea University. The authors would also like to acknowledge the Centre for NanoHealth (CNH) at Swansea University for access to facilities and equipment.

References

Arsenov, P.V., Efimov, A.A. and Ivanov, V.V., 2018. Effect of methods of changing in focusing ratio on line geometry in aerosol jet printing. Key *Engineering Materials*, 779, pp. 159–164. https://doi.org/10.4028/www.scientific.net/KEM.779.159.

Cantù, E., Tonello, S., Abate, G., Uberti, D., Sardini, E. and Serpelloni, M., 2018. Aerosol jet printed 3D electrochemical sensors for protein detection. *Sensors,* 18(11): 3719. https://doi.org/10.3390/s18113719.

Clifford, B., 2017. *Optimisation of aerosol jet deposition for the development of printed electronics*. Ph.D. thesis. Swansea University.

Clifford, B., Beynon, D., Phillips, C. and Deganello, D., 2018. Printed-sensor-on-chip devices – aerosol jet deposition of thin film relative humidity sensors onto packaged integrated circuits. *Sensors and Actuators B: Chemical*, 255(1), pp. 1031–1038. https://doi.org/10.1016/j.snb.2017.08.086.

Goth, C., Putzo, S. and Franke, J.K.H., 2011. Aerosol jet printing on rapid prototyping materials for fine pitch electronic applications. In: *IEEE 61st Electronic Components and Technology Conference (ECTC)*. Lake Buena Vista, FL, USA, 31 May–3 June 2011. IEEE. https://doi.org/10.1109/ECTC.2011.5898664.

Hoey, J.M., Lutfurakhmanov, A., Schulz, D.L. and Akhatov, I.S., 2012. A review on aerosol-based direct-write and its applications for microelectronics. *Journal of Nanotechnology*, 2012: 324380. https://doi.org/10.1155/2012/324380.

Hon, K.K.B., Li, L. and Hutchings, I.M., 2008. Direct writing technology – advances and developments. *CIRP Annals – Manufacturing Technology*, 57(2), pp. 601–620. https://doi.org/10.1016/j.cirp.2008.09.006.

Mahajan, A., Frisbie, C.D. and Francis, L.F., 2013. Optimization of aerosol jet printing for high-resolution, high-aspect ratio silver lines. *ACS Applied Material & Interfaces*, 5(11), pp. 4856–4864. https://doi.org/10.1021/am400606y.

Marquez, G.J., Renn, M.J. and Miller, W.D., 2001. Aerosol-based direct-write of biological materials for biomedical applications. *MRS Online Proceedings Library*, 698: Q5.2.1. https://doi.org/10.1557/PROC-698-Q5.2.1.

Mette, A., Richter, P.L., Hörteis, M. and Glunz, S.W., 2007. Metal aerosol jet printing for solar cell metallization. *Progress in Photovoltaics: Research and Applications*, 15(7), pp. 621–627. https://doi.org/10.1002/pip.759.

Wilkinson, N.J., Smith, M.A.A., Kay, R.W. and Harris, R.A., 2019. A review of aerosol jet printing — a non-traditional hybrid process for micro-manufacturing. *The International Journal of Advanced Manufacturing Technology*, 105, pp. 4599–4619. https://doi.org/10.1007/s00170-019-03438-2.

Zhang, Y., Liu, C. and Whalley, D.C., 2009. Direct-write techniques for maskless production of microelectronics: a review of current state-of-the-art technologies. In: *International Conference on Electronic Packaging Technology & High Density Packaging (ICEPT-HDP '09)*. Beijing, China, 10–13 August 2009. IEEE, pp. 487–503. http://dx.doi.org/10.1109/ICEPT.2009.5270702.

Zhao, D., Liu, T., Zhang, M., Liang, R. and Wang, B., 2012. Fabrication and characterization of aerosol-jet printed strain sensors for multifunctional composite structures. *Smart Materials and Structures*, 21(11): 115008. https://doi.org/10.1088/0964-1726/21/11/115008.

Zöllmer, V., Müller, M., Renn, M., Busse, M., Wirth, I., Godlinski, D. and Kardos, M., 2006. Printing with aerosols: a maskless deposition technique allows high definition printing of a variety of functional materials. *European Coatings Journal*, 07–08: 46.

JPMTR 131 | 2002
DOI 10.14622/JPMTR-2002
UDC 535.3|53.086-028.25

Research paper
Received: 2020-03-23
Accepted: 2020-03-31

The use of infrared and Raman microscopy to characterise the absorption of offset ink in paper

Alexandra Hodes[1,2], Simon Hamblyn[1,2], Matthias Schmidt[3], Ulrike Käppeler[1,2], Andrea Berlich[4], Andrea Prager[5] and Lutz Engisch[1]

[1] Leipzig University of Applied Sciences (HTWK Leipzig), Faculty of Computer Science and Media, Germany
[2] iP[3] Leipzig – Institute for Printing, Processing and Packaging Leipzig at HTWK Leipzig, Germany
[3] ProVIS – Centre for Chemical Microscopy at Helmholtz Centre for Environmental Research GmbH – UFZ / Department of Isotope Biogeochemistry, Germany
[4] Leipzig University of Applied Sciences (HTWK Leipzig), Mathematical-scientific center, Germany
[5] The Leibniz Institute of Surface Engineering (IOM), Germany

alexandra.hodes@htwk-leipzig.de
simon.hamblyn@htwk-leipzig.de
matthias.schmidt@ufz.de
ulrike.kaeppeler@htwk-leipzig.de
andrea.berlich@htwk-leipzig.de
andrea.prager@iom-leipzig.de
lutz.engisch@htwk-leipzig.de

Abstract

Previous studies have detected traces of mineral oils in food packaged in paperboard packaging, with the migration of the ink oil used on the outside of the packaging identified as a potential source of this contamination. This study examined the use of both infrared (IR) microscopy and Raman microscopy to evaluate their use in the detection of mineral oil migration from an offset printing ink through a bespoke set of laboratory made paper hand sheet samples. The IR microscopy was found to be largely unsuitable for this type of investigation due to the low IR reflectance of the materials used in the paper and the ink. Raman microscopy was able to clearly distinguish between the different ink and paper components and therefore characterise the migration within the paper samples. The initial results showed that the use of calcium carbonate pigments as a filler reduced the migration of mineral oil through the paper. For the coated papers, the majority of the mineral oil was detected within same region as the coating. This was in agreement with other studies that have examined the absorption of ink oils into the pore network of calcium carbonate paper coatings.

Keywords: food packaging, migration, mineral oil, paper filler, paper coating

1. Introduction

Printing inks consist of four main ingredients: pigments, binders, solvents and additives. Offset inks could contain mineral oils as a solvent. In the setting and drying process, the oils firstly penetrate into the paper or paper coating. Some papers are coated to improve print quality. The absorption of the ink oils into pigment-based paper coatings has been the subject of much research.

The absorption has been shown to be a function of the pore structure of the coating (Gane, Schoelkopf and Matthews, 2000), the chemistry of the coating (Rousu, Gane and Eklund, 2003) as well as the viscosity, surface tension and polarity of the oils (Tåg, et al., 2013). The absorption is primarily driven by capillary flow (Schoelkopf, et al., 2000), with diffusion into coating components such as latex (Rousu, et al., 2000a; 2000b) also occurring. Small quantities of alkyd and hard resin binders are also absorbed with the oils into the coating (Ström, Gustafsson and Sjölin, 2000). The majority of the binder materials remain on top of the coating, binding the pigment particles to the surface of the paper or paper coating. Due to the random fibre network, the ink absorption into paper is inhomogeneous (Kappel, et al., 2008), but paper-making parameters such as calendering and fibre refining have a strong impact on the absorption characteristics of a paper (Yang, et al., 2005).

The use of mineral oils in offset printing inks has become somewhat controversial in the packaging industry. When the food gets in touch directly with the packaging the use of mineral oil containing offset ink is forbidden. In the food sector, offset inks with vegetable oils are used as solvents. Despite all these measures, mineral oils in foods have still been detected by analysis. Traces of mineral oils have been found in dry foods such as rice, pasta and breakfast cereals (Droz and Grob, 1997). These can accumulate in the body and lead to organ damage (World Health Organisation, 2002; Van Heyst, et al., 2019).

It is widely known that the mineral oil contamination could originate from different sources in the production and delivery system, including from the lubrication oils from the machines used in farming and production; or the batching oils used in the jute bags that are used for transport and storage of products such as cocoa beans, rice and nuts (Moret, Grob and Conte, 1997). Paperboard packaging can contain a large percentage of recycled paper fibres, which were previously printed with offset inks containing mineral oil, for example, newspapers (Biedermann and Grob, 2010; Biedermann, et al., 2011; Vollmer, et al., 2011; Lorenzini, et al., 2010; 2013). If the packaged goods come into direct contact with the packaging, virgin fibres should, therefore, be used.

This investigation was part of a larger study into ink migration. Here we discuss the use of infrared (IR) and Raman microscopy to examine the migration of offset ink components through paper samples and present some initial results for different samples.

2. Methods

2.1 Sample preparation

2.1.1 Paper samples

Initial studies examining offset ink penetration in a paper using commercially available papers proved inconclusive because the exact composition of the papers was unknown. Therefore, for this study, a structured set of hand sheet paper samples were produced using a Rapid Köthen Sheet former. Four different paper types were produced, all using the same type of bleached chemi-thermo-mechanical-pulp (BCTMP) fibres, each with a different combination of sizing and calcium carbonate filler content. In addition, different types of subsequent processing such as calendaring and coating were also used. The coating consisted of calcium carbonate pigments dispersed in a carboxyl--styrene-butadiene based latex binder.

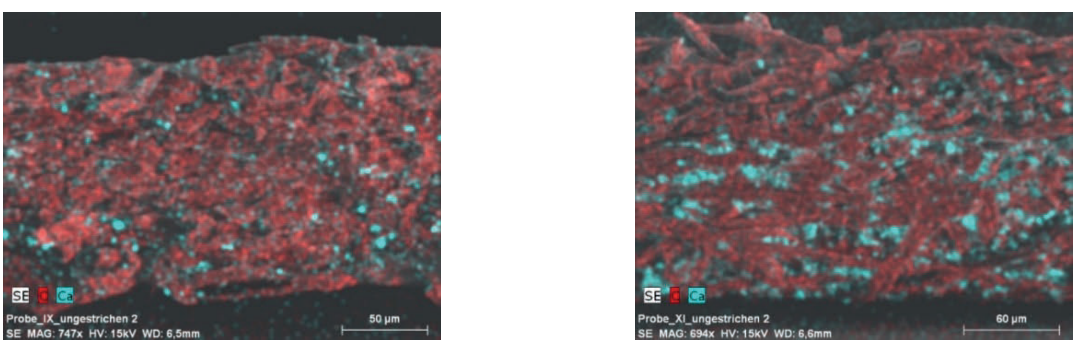

a) b)

Figure 1: SEM/EDX pictures of uncoated paper with (a) low quantity of filler, (b) high quantity of filler

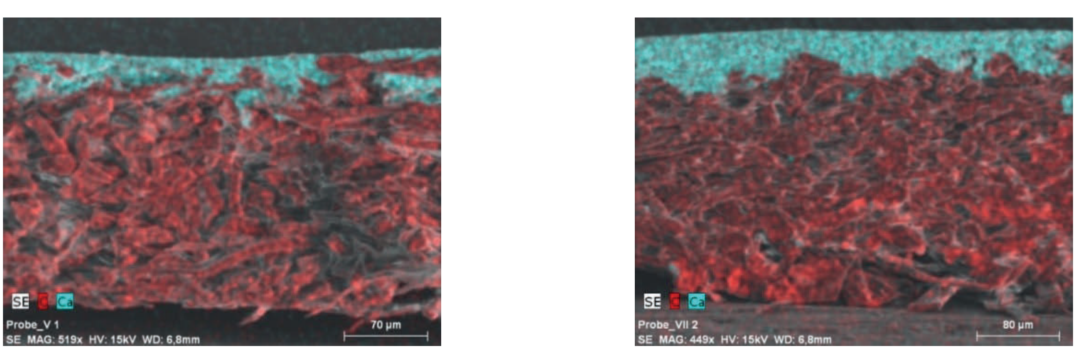

a) b)

Figure 2: SEM/EDX pictures of paper without filler with (a) single coating, (b) double coating

One potential problem with laboratory crafted hand sheets is an uneven retention of fillers and fibres. Therefore, to control the quality, imaging with Scanning Electron Microscopy and Energy Dispersive X-Ray Analysis (SEM/EDX) of unprinted paper-cross-sections were carried out. Figure 1 shows a comparison between two uncoated paper samples: one with a low quantity of filler and the other with a higher quantity of filler. The calcium carbonate filler shows up as light blue in the SEM/EDX images, while the fibres have a red colour. In both types of samples, the filler was relatively evenly distributed throughout the fibre matrix.

Figure 2 shows a comparison of two papers, one with a single and the other with a double-layer coating, both types of sample did not contain fillers. Since calcium carbonate was also used in the coating material, this also shows up as light blue in the SEM/EDX images.

2.1.2 Printing ink

For the print samples, a bespoke offset printing ink was used. This ink was comparable to typical sheet-fed ink containing mineral oil but did not contain additives such as wax. The ink was a process cyan containing copper phthalocyanine pigments. A suitable colour was needed that provided a strong colour contrast on the paper. While black would have provided the best visual contrast on the white paper, the inorganic carbon black pigments were not suitable for vibration spectroscopic methods because of their absorption characteristics. Cyan provided both a good visual contrast and also produced a strong Raman signal. In addition, the main ink's components such as the pigments, binder, mineral oil and the alkyd resin were provided as individual reference components for use in the IR and Raman spectroscopy.

2.1.3 Preparation of the samples

The laboratory paper samples (hand sheets) were printed with a 100 % solid tone on one side, using a printability tester (Prüfbau printability tester, Germany). For each sample, a controlled and constant amount of the ink was used. The same speed and nip pressures were used to produce each sample. For IR and Raman analysis, thin slices, named microtomes, are a commonly used approach to prepare samples. This involves first embedding the printed paper samples in a resin. When the resin is solidified, very thin slices are cut using a microtome blade. This approach was tried with both methacrylate and epoxy resins, but in both cases resulted in the ink bleeding. Therefore, in order to prepare the samples, a method was developed, where 10 mm × 10 mm layered blocks were made. These consisted of alternating layers of the printed paper samples with layers of polytetrafluoroethylene (PTFE) in between. The PTFE was used because it provided distinguishable IR and Raman spectra compared to the other materials. These layered blocks were then sandwiched between two thicker polyvinyl chloride (PVC) plates (Figure 3).

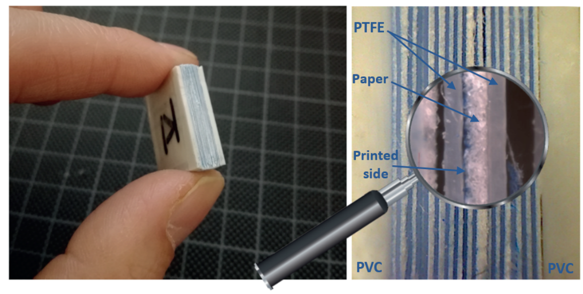

Figure 3: Paper-film-sandwich block, stabilized outside with two thick PVC-films

For the IR spectrometry, microtomes were produced from these sandwich blocks. One advantage of the Raman spectrometer over the IR spectrometer was that it could work with thicker samples; therefore, the sandwich blocks could be used directly in the instrument, eliminating the need to produce microtomes.

2.2 Sample characterisation

Methods were developed using both IR microscopy and Raman microscopy to characterise the cross-sections of the printed paper samples. Because the main area of interest of this study was to detect mineral oil migration in packaging, the printed samples were stored for a period of four months before characterisation, which would correspond to the lifecycle of a typical paper-based packaging.

2.2.1 IR microscopy

An infrared microscope consists of an IR spectrometer, an infrared detector, and an optical microscope. A Perkin Elmer Spectrum One FTIR Spectrometer with an Autoimage Microscope was used for generating infrared reflection-absorption spectroscopic (IRRAS) line scans from the microtome cuts of the printed paper sections. The results from a typical line scan are shown in Figure 4.

A total of 15 spectra with a repeatability of 64 scans per spectrum were recorded in each line scan. Measurement of the location of the individual printing ink and paper components were made by comparing the line scan spectra with the reference spectra of the base paper, paper coating, and ink as well as the individual ink and paper components to calculate a correlation coefficient.

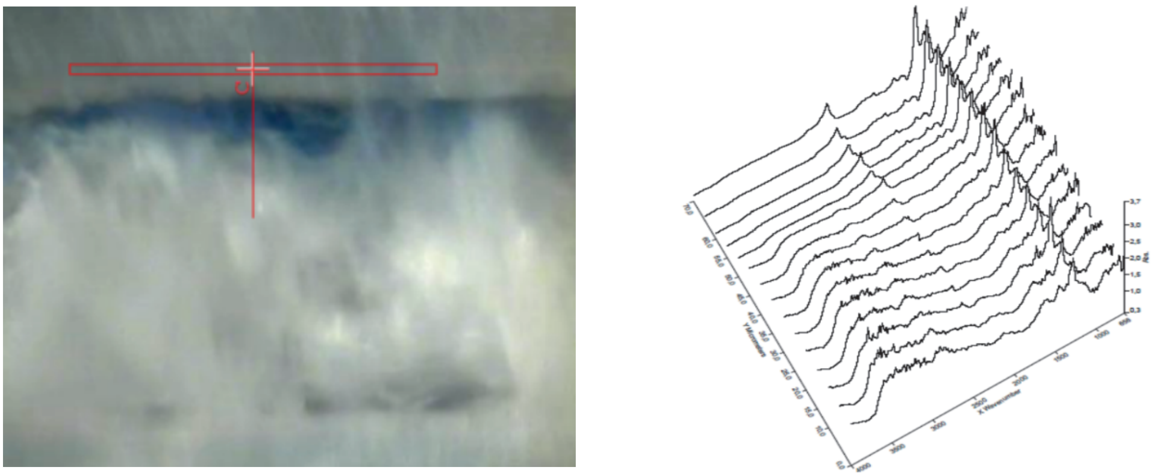

a) b)

Figure 4: Line scan of the paper cross-section (a) and typical line scan spectra (b)

2.2.2 Raman microscopy

For Raman microscopy, a confocal Raman microscope alpha 300 R+ from WITec was used. From initial experiments, with different laser types, it was found that a green Nd:YAG Laser (λ = 532 nm) produced repeatable results in detecting the ink and paper components with a high signal-to-noise ratio. Furthermore, wavenumbers up to 3 700 cm^{-1} could be reproduced. As the excitation laser radiation from the Raman spectrometer is much more intense than the resultant Raman scattering from the sample, a notch filter was used to prevent this excitation radiation from reaching the CCD detector and clouding the spectrum. A very narrow-band filter was used, so that the wavenumbers from the green laser (until approximately 70 cm^{-1}) were absorbed, therefore allowing the wavenumbers above approximately 80 cm^{-1} to be used for analysis.

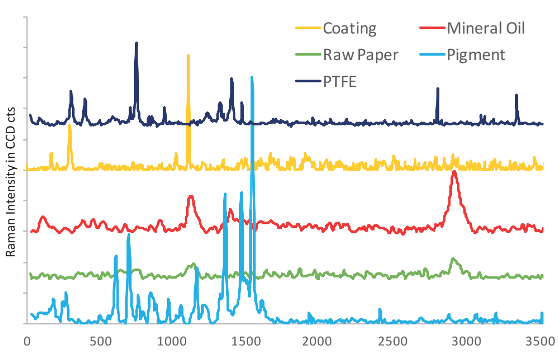

Figure 5: Relevant Raman spectra of the individual components

The individual Raman spectra of each of the main ink and paper components in the preliminary sample were measured to generate reference spectra in order to identify the unique signature wavenumber peaks of each component, which could then be used later to detect its presence in the printed paper samples. The Raman spectra of the main components are shown in Figure 5.

The pigment provided the clearest and most intense signal with few overlaps with those of the other materials. However, differentiation between the Raman spectra of the paper coating, mineral oil, and base paper was more difficult. All three materials produced a signal peak at approximately 1 100 cm^{-1}. The raw paper provided only two usable peaks at approximately 1100 cm^{-1} and 2 900 cm^{-1}. The mineral oil also provided peaks in these regions. For this reason, the peak for the mineral oil band at 96 cm^{-1} was used for the evaluation. The mineral oil gives a significant signal in this area, which was absent in the spectra of the other materials (Figure 6). According to Cates, Strauss and Snyder (1994) it could be a CC torsion vibration.

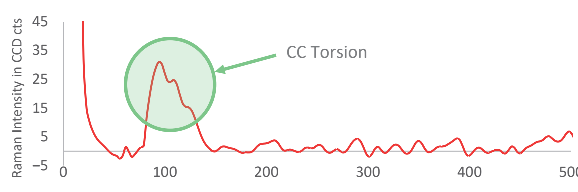

Figure 6: Raman spectrum of the mineral oil from a green laser (only the portion up to 500 cm^{-1} is shown)

Using the Raman microscope, the entire paper cross-section was measured during an image scan. A typical measurement region is shown in Figure 7.

Filters with different wavenumber bands were then created within the analysis software, in order to identify the different components based on the characteristic peaks determined from the Raman spectra.

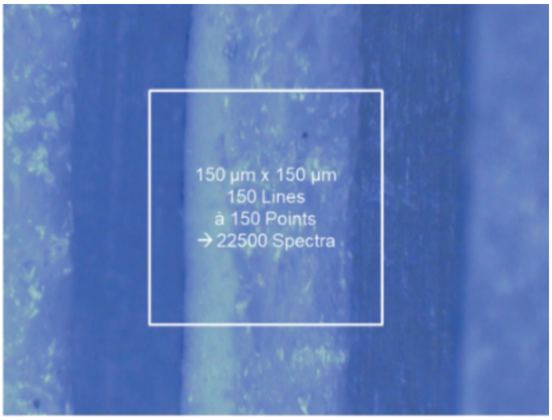

Figure 7: Magnification of sandwich block with a selected region for a Raman image scan

Examples of the most relevant filtered images are shown in Figure 8.

To measure the depth within the samples at which the different components were found, the filtered images were first vertically aligned to minimise skew, and then transformed into greyscale images. An example of a greyscale image for the filter selected for the pigment particles (1517 cm^{-1} to 1552 cm^{-1}) is shown in Figure 9.

The freeware software GNU Octave was then used to evaluate the average greyscale values as a function of the distance in *x*-direction. Figure 10 shows the plot of the greyscale values with the confidence interval for the cyan pigment component generated from image in Figure 9.

The plots of the five types of filtered images (PTFE, pigment, coating, mineral oil and base paper) have been combined into a single diagram shown in Figure 11.

For this preliminary sample, approximately the first 7 µm of the image was the PTFE film. This was followed by the pigment up to approximately 14 µm. The coating layer reached approximately to 40 µm.

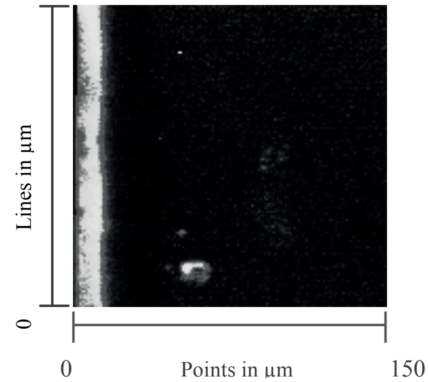

Figure 9: Greyscale image of the Pigment filter (1517 cm^{-1} to 1552 cm^{-1})

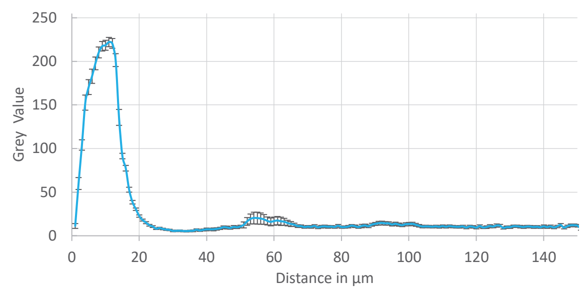

Figure 10: Average greyscale as a function of distance with error bars of the pigment distribution

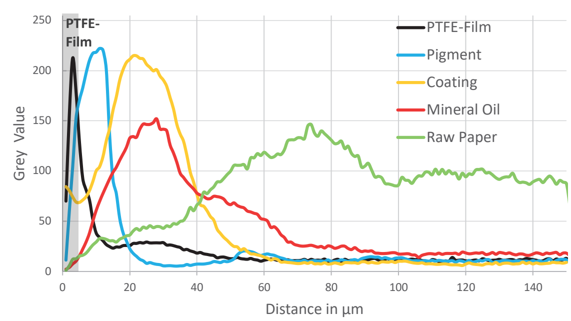

Figure 11: Results of the grey value intensity distributions of the individual materials of the preliminary sample of printed coated paper without filler

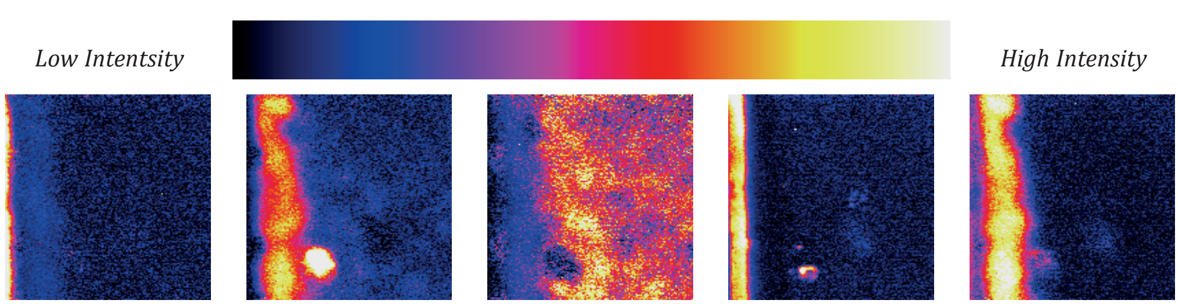

PTFE-Film (716 cm^{-1} to 750 cm^{-1}) | *Mineral Oil (93 cm^{-1} to 98 cm^{-1})* | *Raw Paper (1101 cm^{-1} to 1130 cm^{-1})* | *Pigment (1517 cm^{-1} to 1552 cm^{-1})* | *Paper Coating (270 cm^{-1} to 310 cm^{-1})*

Figure 8: Filtered images of a Raman image scan of a printed and coated paper without filler

There was some overlap between the pigment and the coating layer, which could be due the pigment penetrating slightly into the coating surface or due to the unevenness of the coating surface topography. It is also possible that the ink contained some $CaCO_3$ as filler. The mineral oil seems to be mostly contained within the coating layer. For this sample, the cyan pigment and mineral oil penetrated to approximately 65 µm in one area, due to a probable flaw in the coating layer (Figures 8, 9, 10). Otherwise the migration of the mineral oil would have stopped at 40 µm.

All of the filtered images from all paper combinations were processed using this approach.

3. Results and discussion

3.1 Results of the IR microscopy

Figure 12 shows a typical result of a correlation analysis between the IR reference spectra from the IR-spectrometry measurements and the line scan from the IR microscope, shown here for the same example of the printed coated paper.

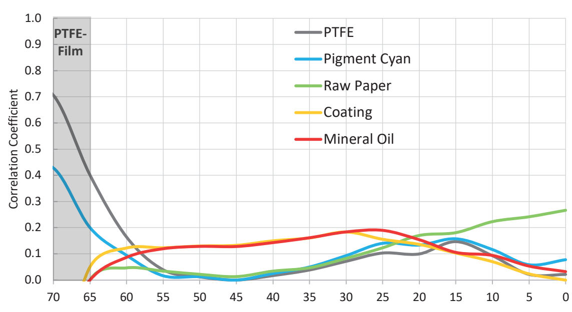

Figure 12: Result of the correlation analysis for the sample of printed coated paper without filler

Also here the mineral oil seemed to be contained almost entirely within the paper coating – approximately also 40 µm penetration depth, with reduced further penetration into the fibre network. This is a possibility, based on the findings of other studies (Rousu, Gane and Eklund, 2003; Rousu, et al., 2000a; Ström, Gustafsson and Sjölin, 2000).

With IR microscope, only relatively low reflectance intensities from the line scan spectra could be detected. Despite the use of thin microtome samples and special reflective slides, too much of the IR radiation was absorbed inside the sample, resulting in very low correlation coefficients for the ink and paper components. Also, the 5 µm aperture of the instrument did not provide enough resolution to accurately determine the migration depth. For these reasons, IR microscopy was deemed to be unsuitable for this type of study.

3.2 Results of the Raman microscopy

The results from the Raman microscope showed no such problems. A typical result is shown in Figure 13 for an unsized, uncoated paper without filler. For the uncoated papers, without fillers, the mineral oil was detected throughout the complete fibre network. These also showed a high concentration of pigments on or near the paper surface, with some penetration into the fibre network to an approximate depth of 30 µm. High levels of the mineral oil were detected throughout the entire depth of the paper, therefore showing that the mineral oil from the ink had migrated through the paper.

For the uncoated papers that also contained fillers, a high concentration of mineral oil was detected in the region near to the paper surface, which shows that the calcium carbonate particles acted as a brake to hinder the oil migration. A typical greyscale filter images for

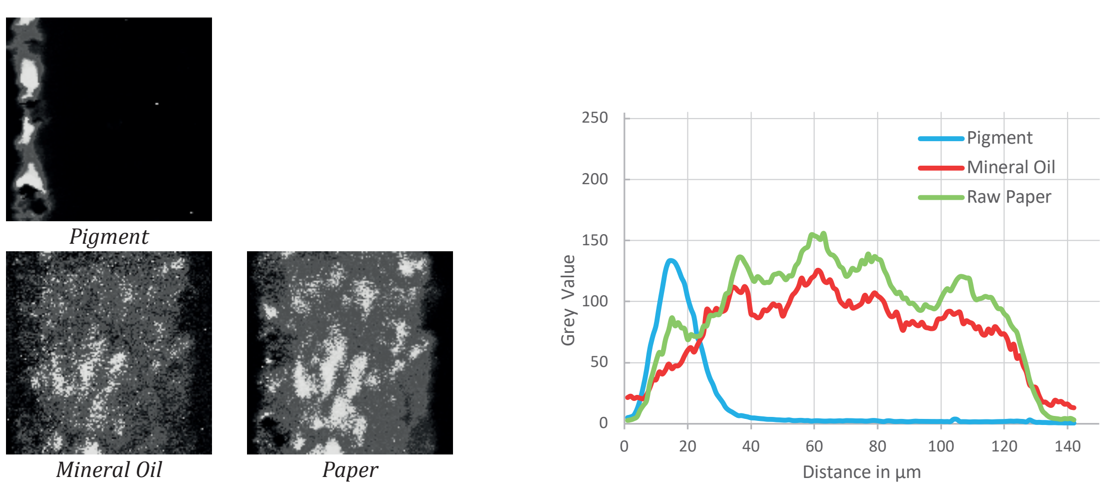

Figure 13: Greyscale filter images and plots from the printed cross-section of an unsized, uncoated paper without filler

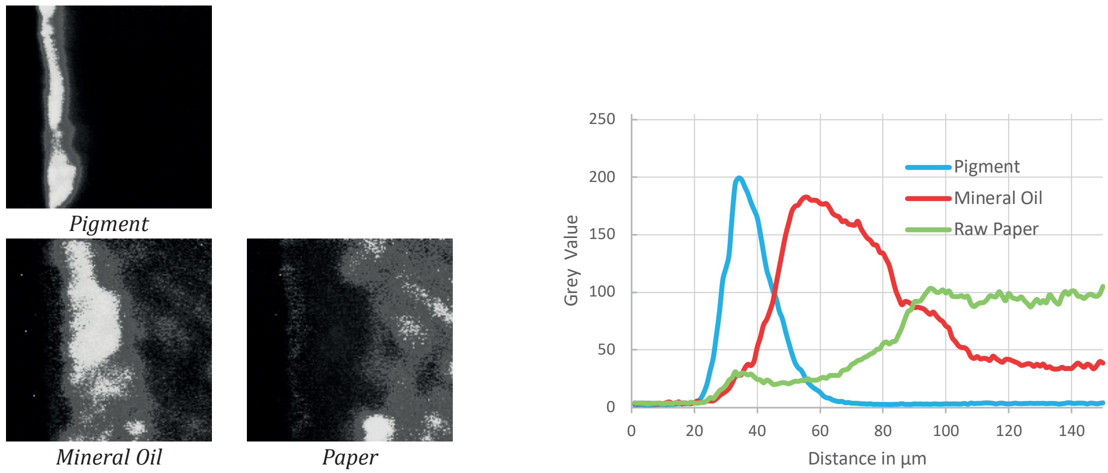

Figure 14: Greyscale filter images and plots from the printed cross-section of an uncoated paper with filler

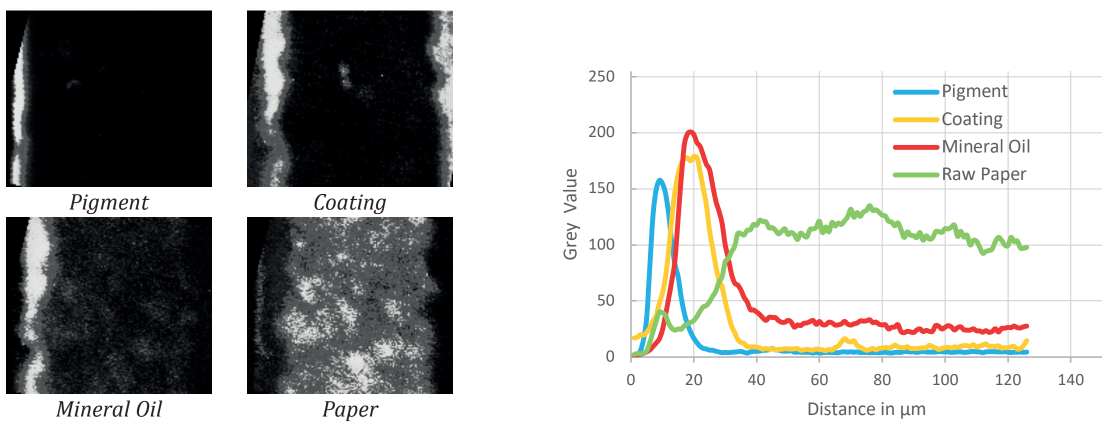

Figure 15: Greyscale filter images and plots from the printed cross-section of a coated paper

the pigment, mineral oil and raw paper and subsequent average intensity plot for a printed and uncoated paper with filler are shown in Figure 14.

For the coated papers, the bulk of the mineral oil was detected within the paper coating, with comparatively little oil detected within the paper fibre network (Figure 15).

4. Conclusions

Methods were developed using IR microscopy and Raman microscopy to characterise the distribution of offset printing ink components in paper cross-sections. IR microscopy proved to be unsuitable for this type of study because the intensity of the reflectance spectra was ultimately too low to quantify the amount of mineral oil and other materials present within the paper samples. Also, due to the limited spatial resolution of the instrument, it was not possible to accurately quantify the depth of the migration. Raman microscopy proved to be more suited to this application. With carefully selected filters based on characteristic peaks in the Raman spectra, it was possible to differentiate the different components and therefore to analyse the penetration depth of mineral oil in the base paper. The initial results showed that in the papers without calcium carbonate fillers and/or coatings, the high concentrations of mineral oil from the printing ink were found throughout the entire paper structure and therefore could potentially reach a product inside of the packaging. Migration was greatly reduced with the inclusion of fillers. The amount of mineral oil detected in the fibre network of the coated papers was relatively low, with high concentrations of the mineral oil detected within the layer of the paper coating. These results were in-line with the findings of other studies (Rousu, Gane and Eklund, 2003; Rousu, et al., 2000a; Ström, Gustafsson and Sjölin, 2000). However, since mineral oil was still detected within the paper fibre network of the coated papers albeit in lower concentrations it is highly feasible that over time the mineral oil from a printing ink could migrate through a coated paper based packaging and reach the content inside.

Acknowledgements

We gratefully acknowledge Prof. Dr. rer. nat. habil. Holger Zellmer for the provision of the GNU Octave script for the image analysis of the filter images (intensity maps) for calculating the grey values and the standard deviation. We also would like to thank Dr. rer. nat. Yalda Davoudpour for her support with the Raman microscope. The research was co-funded by the German Federal Ministry of Education and Research and the Saxon State Ministry of Arts, Culture and Tourism as part of the project “Smart University Grid Saxony[5]”, subproject “Co-Creation Lab Surface Engineering”.

References

Biedermann, M. and Grob, K., 2010. Is recycled newspaper suitable for food contact materials? Technical grade mineral oils from printing inks. *European Food Research and Technology*, 230(5), pp. 785–796. https://doi.org/10.1007/s00217-010-1223-9.

Biedermann, M., Ingenhoff, J.-E., Barbanera, M., Garbini, D. and Grob, K., 2011. Migration of mineral oil into noodles from recycled fibres in the paperboard box and the corrugated board transport box as well as from printing inks: a case study. *Packaging Technology and Science*, 24(5), pp. 281–290. https://doi.org/10.1002/pts.937.

Cates, D.A., Strauss, H.L. and Snyder, R.G., 1994 Vibrational modes of liquid n-alkanes: simulated isotropic Raman spectra and band progressions for C_5H_{12}–$C_{20}H_{42}$ and $C_{16}D_{34}$. *The Journal of Physical Chemistry*, 98(16), pp. 4482–4488. https://doi.org/10.1021/j100067a041.

Droz, C. and Grob, K., 1997. Determination of food contamination by mineral oil from printed cardboard using on-line coupled LC-GC-FID. *Zeitschrift für Lebensmitteluntersuchung und -Forschung A*, 205(3), pp. 239–241. https://doi.org/10.1007/s002170050158.

Gane, P.A.C., Schoelkopf, J. and Matthews, G.P., 2000. Coating imbibition rate studies of offset inks: a novel determination of ink-on-paper viscosity and solids concentration using the ink tack force-time integral. In: *2000 TAPPI International Printing & Graphic Arts Conference Proceedings*. Savannah, GA, USA, 1–4 October 2000. Atlanta, GA, USA, TAPPI Press, pp. 71–88.

Kappel, C., Hirn, U., Donoser, M. and Bauer, W., 2008. Measurement of printing ink penetration in uncoated papers and its influence on print quality. In: *94th Annual Meeting, Pulp and Paper Technical Association of Canada*. Montreal, QC, Canada, 6–7 February 2008. Montreal: PAPTAC, pp. 539–542.

Lorenzini, R., Biedermann, M., Grob, K., Garbini, D., Barbanera, M. and Braschi, I., 2013. Migration kinetics of mineral oil hydrocarbons from recycled paperboard to dry food: monitoring of two real cases. *Food additives & contaminants: Part A*, 30(4), pp. 760–770. https://doi.org/10.1080/19440049.2013.766765.

Lorenzini, R., Fiselier, K., Biedermann, M., Barbanera, M., Braschi, I. and Grob, K., 2010. Saturated and aromatic mineral oil hydrocarbons from paperboard food packaging: estimation of long-term migration from contents in the paperboard and data on boxes from the market. *Food additives & contaminants: Part A*, 27(12), pp. 1765–1774. https://doi.org/10.1080/19440049.2010.517568.

Moret, S., Grob, K. and Conte, L.S., 1997. Mineral oil polyaromatic hydrocarbons in foods, e.g. from jute bags, by on-line LC-solvent evaporation (SE)-LC-GC-FID. *Zeitschrift für Lebensmitteluntersuchung und -Forschung A*, 204(3), pp. 241–246. https://doi.org/10.1007/s002170050071.

Rousu, S., Gane, P. and Eklund, D., 2003. Distribution of offset ink constituents in paper coating and implications for print quality. In: *8th TAPPI Advanced Coating Fundamentals Symposium*. Chicago, IL, USA, 8–10 May 2003. Atlanta, GA, USA: TAPPI Press, pp. 125–136.

Rousu, S.M., Gane, P.A.C., Eklund, D.E. and Spielmann, D.C., 2000a. Differential absorption of offset ink components on coated paper. In: *2000 TAPPI International Printing & Graphic Arts Conference Proceedings*. Savannah, GA, USA, 1–4 October 2000. Atlanta, GA, USA, TAPPI Press, pp. 55–70.

Rousu, S., Gane, P., Spielmann, D. and Eklund, D., 2000b. Separation of off-set ink components during absorption into pigment coating structures. *Nordic Pulp & Paper Research Journal*, 15(5), pp. 527–535. https://doi.org/10.3183/npprj-2000-15-05-p527-535.

Schoelkopf, J., Gane, P.A.C., Ridgway, C.J. and Matthews, G.P., 2000. Influence of inertia on liquid absorption into paper coating structures. *Nordic Pulp & Paper Research Journal*, 15(5), pp. 422–430. https://doi.org/10.3183/npprj-2000-15-05-p422-430.

Ström, G., Gustafsson, J. and Sjölin, K., 2000. Separation of ink constituents during ink setting on coated substrates. In: *2000 TAPPI International Printing & Graphic Arts Conference Proceedings*. Savannah, GA, USA, 1–4 October 2000. Atlanta, GA, USA, TAPPI Press.

Tåg, C.-M., Toiviainen, M., Ridgway, C., Juuti, M. and Gane, P.A.C., 2013. Dynamic ink oil absorption in a pigmented porous coating medium studied by near-infrared diffuse reflectance spectroscopy. *Transport in Porous Media*, 99(1), pp. 145–160. https://doi.org/10.1007/s11242-013-0178-2.

Van Heyst, A., Goscinny, S., Bel, S., Vandevijvere, S., Mertens, B., Elskens, M. and Van Hoeck, E., 2019. Dietary exposure of the Belgian population to mineral oil. *Food additives & contaminants: Part A*, 37(2), pp. 267–279. https://doi.org/10.1080/19440049.2019.1684573.

Vollmer, A., Biedermann, M., Grundböck, F., Ingenhoff, J.-E., Biedermann-Brem, S., Altkofer, W. and Grob, K., 2011. Migration of mineral oil from printed paperboard into dry foods: survey of the German market. *European Food Research and Technology*, 232(1), pp. 175–182. https://doi.org/10.1007/s00217-010-1376-6.

World Health Organisation, 2002. *Evaluation of certain food additives: fifty-ninth report of the Joint FAO/WHO Expert Committee on Food Additives*. Geneva, Switzerland: WHO.

Yang, L., Fogden, A., Pauler, N., Sävborg, Ö. and Kruse, B., 2005. A novel method for studying ink penetration of a print. *Nordic Pulp & Paper Research Journal*, 20(4), pp. 423–429. https://doi.org/10.3183/npprj-2005-20-04-p423-429.

TOPICALITIES

Edited by Markéta Držková

CONTENTS

News & more

Recent patents related to electrically conductive printing inks

For the third time, the spring JPMTR issue brings a brief review of the patents published during last year. This time, the focus is on the 2019 European and U.S. patents classified in the subgroup of electrically conductive inks. From almost a hundred assignees, the following text is limited to the companies with four or more patents.

Hewlett-Packard

Eleven patents from this selection were granted to HP Indigo. While the names of US 10,514,625 B2 Electrophotographic ink including a volatile fragrance and EP 2 875 080 B1 Polymerically coated metallic pigment particles, method for providing them and electrostatic inks are sufficiently informative, seven patents are entitled simply Electrostatic ink composition(s). Of these, US 10,401,751 B2 details the composition of cyan electrostatic ink, EP 3 137 561 B1 presents the composition containing a sulfosuccinate salt as a charge director and a non-polymeric, non-fatty acid to reduce the sensitivity of the particle conductivity to the concentration of charge director. Further, US 10,289,018 B2 deals with the pigment comprising mica coated with titanium dioxide and an additional metal oxide and EP 3 295 252 B1 with white pigment particles having a basic species on their surface. Another one, US 10,344,175 B2, describes the electrostatic ink composition with a fluorescent pigment, which constitutes typically about 10–50 % of the total solids. Finally, US 10,416,583 B2 and EP 3 327 093 B1 deal with the electrostatic ink composition containing an elongate conductive species, typically based on carbon nanotubes. The remaining two HP Indigo patents published in 2019 are EP 2 855 605 B1 Electrostatic inks and printing, which describes a method of producing an electrostatic ink composition, and US 10,437,167 B2 Ink composition, which presents the liquid electrophotographic ink composition containing a terpene phenolic resin as a tackifier to improve the adhesion of the ink composition to the substrate.

In addition, three patents were granted to Hewlett-Packard Development Company: US 10,377,909 B2 Inks including segment copolymer grafted pigments via azide chemistry, which describes also the use of such electronic ink in an electronic display, EP 3 039 088 B1 Electronic inks, specifying the electronic ink together with a method for making it and its use in a display element, and EP 2 951 246 B1 Electrostatic ink compositions methods and print substrates, presenting a composition employing a pearlescent, non-metallic pigment to produce prints with a metallic appearance.

Xerox Corporation

From six patents granted to Xerox, one is related to the field of inkjet printhead manufacturing: US 10,166,777 B2 Method of forming piezo driver electrodes, which employs inkjet printing of a conductive material. The other patents describe the composition of inks and layers for printed electronics applications. One of these is US 10,246,599 B2 Ink composition and method of determining a degree of curing of the ink composition, where the change in colour between the uncured and cured state of the ink containing silver

What is uneasy and what is special about these incredibly challenging times

Keeping the focus on the field of print and media technology, the pandemic breakout impacts are most visibly manifested by all events that have been postponed or cancelled – or are expected to be. The short overview of the changes and tentative dates, as announced to date, is presented in the Events section. Many difficulties in the industry are being caused by travel and transport restrictions, requirements for social distancing, quarantine and other necessary measures taken in more and more countries across the world. In a few countries, newspaper printing is suspended. Now it is too soon to count losses as the situation changes almost daily. However, the adverse circumstances affect the industry in many ways – not only directly, causing a decrease in production and sales volume, but also through a falling demand for advertisement, and the allied loss of customer confidence.

Nevertheless, on the bright side, all kinds of media and communication channels keep people informed and help them to cope with isolation, as well as to advise on implementing home office and distance education. Where needed, both academia and industry are stepping in to provide the capacity of advanced 3D printers to produce protective equipment, parts such as valves and, if approved, also ventilators. Software companies support the people who are confined to stay at home without the access to a computer or a licence server at work by providing them with the temporary licences or by prolonging the trial period, e.g. to 90 days in the case of the Serif Affinity suite. The same or even more applies to support for students and teachers, having temporary at-home access to Adobe Creative Cloud or QuarkXPress, for example. Also, some companies now offer free access to their e-learning resources, such as Esko and Enfocus.

Recent news from the Ghent Workgroup

In December 2019, GWG released the new specification for the Sign & Display market. It incorporates the concepts of viewing distance, which is connected with the requirements on image resolution and can range from one to tens of metres, and scaling factor, which takes into account files created in a smaller scale compared to the final printed size to overcome the limitations of some applications. Due to the number of wide-gamut output devices in use for large-format printing, this GWG specification as the first one allows the use of ICC-based colour spaces for all elements within a PDF document.

In March 2020, the Ghent Workgroup presented a new webinar on native transparency and its use. The Q&A webinar is scheduled for 19 May.

ABB solutions for the newspaper industry

With more than a hundred years of experience in the newspaper printing industry, ABB is a supplier of press controls, drives, automation solutions and integrated production management systems. For older presses, ABB offers a range of modular retrofit solutions, successfully implemented on dozens of presses from all major manufacturers. Some systems can be commissioned even without taking the press out of production. Last year, the modernisation projects included the drives retrofit for Mitsubishi presses and the press controls retrofit on Wifag and KBA Commander presses. The ABB production management systems cover the entire newspaper production process – from the roll handling, over the production and press control, to the management of inserts and distribution planning, with a complete overview and control provided by the solutions for resource management and planning across one or more print sites as well as for plant-wide online monitoring, reporting and analysis.

flakes is achieved through the addition of silver nanoparticles. Conductive inks containing nanoparticles are described also in US 10,214,655 B2 Metal nanoparticle ink dispersion and US 10,492,297 B2 Hybrid nanosilver/liquid metal ink composition and uses thereof, whereas US 10,208,224 B2 Interlayer composition for electronic printing and EP 3 296 364 B1 UV curable interlayer composition for printed electronics application present the methods to improve the adhesion of the printed conductive layer to the substrate.

The patents related to the electrically conductive inks granted to other companies

Looking at the remaining patents from this 2019 selection, two companies claimed the inventions dealing with compositions containing silver. Four patents of Dowa Electronics Materials include the two on dispersing silver nanoparticles; in EP 2 946 856 B1 Silver fine particle dispersion liquid, silver is coated with an amine, while in US 10,350,679 B2 Fine silver particle dispersing solution, it is coated with an organic acid or its derivative. In the case of particle size about 1 μm, which is considered in US 10,272,490 B2 Silver powder, method for producing same, and hydrophilic conductive paste, the surface of the silver contains phytic acid. The last one is EP 3 118 272 B1 Method for producing silver nanowire ink, silver nanowire ink, and transparent electroconductive coating film. Different approaches to provide a coating or pattern with (nano)particles of silver are presented in four patents granted to Eastman Kodak Company. These are US 10,174,425 B2 Non-aqueous compositions and articles using stannous alkoxides, with a photocurable component including a free radical photoinitiator, US 10,214,657 B2 Silver-containing compositions containing cellulosic polymers, US 10,370,515 B2 Silver-containing non-aqueous composition containing cellulosic polymers and US 10,487,221 B2 Photosensitive compositions containing silver ion α-oxy carboxylate-oxime complexes.

Dealing with different materials, the LG Chem patents are US 10,240,057 B2 Conductive polymeric ink composition, presenting a neutralised poly(3,4-ethylenedioxythiophene) poly(styrene-sulfonate) (PEDOT:PSS) aqueous dispersion, US 10,294,379 B2 Ink composition for organic solar cell and method for producing organic solar cell using same, US 10,418,498 B2 Method of preparing metal chalcogenide nanoparticles and method of producing light absorption layer thin film based thereon and US 10,435,571 B2 Method for preparing carbon nanotube, and dispersion composition of carbon nanotube.

The patents of Nissan Chemical Corporation (formerly Nissan Chemical Industries) include US 10,266,701 B2 Composition for forming protective film for transparent conductive film, US 10,385,229 B2 Non-aqueous ink compositions containing metallic nanoparticles suitable for use in organic electronics (with polythiophenes that may be doped or undoped), US 10,407,581 B2 Non-aqueous compositions having sulfonated polythiophenes suitable for use in organic electronics and US 10,435,579 B2 Compositions containing hole carrier materials and fluoropolymers, and uses thereof.

Finally, the Northwestern University patents deal with the use of graphene. These comprise US 10,494,536 B2 Methods for preparation of concentrated graphene compositions and related composite materials, US 10,350,329 B2 Graphene-based ink compositions for three-dimensional printing applications, US 10,280,317 B2 Enhanced conductivity, adhesion and environmental stability of printed graphene inks with nitrocellulose and, jointly with the University of Minnesota, US 10,479,905 B2 High-resolution patterning of graphene by screen and gravure printing for highly flexible printed electronics.

Bookshelf

A Companion to the History of the Book

After more than ten years since the first publication, this text on the history of the book was published in a second edition as a two-volume set with a completely revised, updated and expanded content. The text provides a comprehensive overview of the subject, supported by many illustrative examples and case studies.

The contributions of over sixty authors are organised into six parts. The first part that brings an overview of bibliography, textual scholarship and the uses of quantification and reveals how readers used their books now also introduces palaeography and codicology and presents new histories of literacy. Further, it includes the chapters dealing with paper, type and typography, printing, binding, archives and paperwork. The following two parts review the history of the book. Part II covers the manuscript culture in Europe and the Middle East – from the clay tablet book in Sumer, Assyria and Babylonia and the papyrus roll in Egypt, Greece and Rome, over the folded codex form of the book, to parchment and paper books in later medieval Europe. Part III then describes the book in China, Japan, Korea and Vietnam, South Asia, Latin America and the Hebraic book, with new chapters exploring the book in Africa, Canada and Australasia, as well as the Slavic book and books in Arabic Script.

The second volume starts with Part IV that reviews the changes due to the invention of printing with movable type, the creation of new commercial models and the evolution of the book trade in the following centuries, covering the situation in Britain, continental Europe and North America, especially in the United States. It discusses the industrialisation and globalisation of the book, along with its increasing accessibility thanks to decreasing price. This part also reflects the important changes in the publishing industry that were connected with international copyright protection and later with digitalisation. The last two chapters outline the changes in the global book market from 1970 to 2015 with respect to producers and consumers.

Beyond the book, the chapters in the fifth part deal with periodicals, the importance of the so-called ephemera printed items preserved mostly thanks to collectors, various non-textual uses of books, the book as art, the new textual technologies and the new topics, which include the history of scientific publications, maps and music printing. Finally, Part VI addresses the development of the concept of copyright, the history of authorship, writing, lexicography and dictionaries, as well as the role of book collecting and libraries. One chapter also examines conceptions of obscenity and attitudes toward censorship. The concluding chapter book sums up the changes brought by the advances in technology – today a book can be read in both printed and digital form, digital printing enables print on demand and self-publishing. As a result, more books are published than ever before.

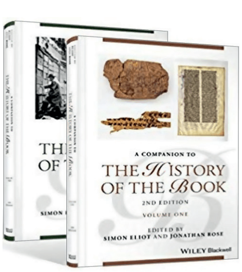

Editors: Simon Eliot, Jonathan Rose

Publisher: Wiley-Blackwell
2nd ed., November 2019
ISBN: 978-1-119-01817-9
976 pages
Hardcover
Available also as an eBook

Field Guide to Colorimetry and Fundamental Color Modeling

Author: Jennifer D. T. Kruschwitz

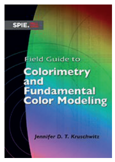

Publisher: SPIE Press
1st ed., August 2018
ISBN: 978-1510621237
126 pages
Softcover
Also as an eBook

Intended for the practising engineer or scientist, the guides published in this SPIE series are written to include the key information in a given field. The pages of this one cover colour matching experiments, the 1931 CIE colour space, colour terminology, display colour gamuts, colour order systems, uniform colour spaces, colour difference equations, basic chromatic adaptation, colour equivalency mapping, colour measurement and colour modelling, printing models and colour management, with the fundamental colorimetric data and additional equations in the appendix.

Coming of Age
The Center for Imaging Science at Rochester Institute of Technology

Author: John R. Schott

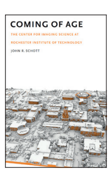

Publisher: RIT Press
1st ed., October 2019
ISBN: 978-1939125651
264 pages, 141 images
Softcover

In this book, John Schott, Professor Emeritus at the Rochester Institute of Technology, chronicles three decades of imaging science at RIT. Documenting all milestones and highlighting the positive synergy of research and education, the text describes the very beginnings, the formation of the Center for Imaging Science and the development of RIT's first doctoral programme, as well as the evolution towards becoming a recognised research facility in the following years. Both the main part and appendices in the second half of the book are richly illustrated with archival photographs.

Billmeyer and Saltzman's Principles of Color Technology

As for the third edition of this book, Roy Berns has substantially revised and updated the text after two decades to reflect all important advancements in colour theory and technology, while keeping the original informal style and explaining the concepts together with the related quantities and equations. The first chapter deals with the physical properties of colours. After a short introduction of the book, the author explains the spectrum, light sources and the interaction of light with the conventional materials through transmission, reflection, absorption, surface and internal scattering. The chapter also describes the difference between dyes and pigments and spectral characteristics of conventional materials. The remaining sections present the materials with specific behaviour, namely the fluorescent, gonio-apparent, photochromic and thermochromic ones. The chapter on colour perception and spatial vision covers trichromacy, adaptation, compression, opponency and observer variability. It is followed by an overview of existing systems used for visual colour specification and the chapters dealing with the colorimetry and specification of colour quality, including the colour-appearance models and colour-difference formulas. Two chapters then present the considerations important when measuring colour and material appearance and choosing illuminants used for lighting, while the next two ones discuss the metamerism and optical modelling of coloured materials. The last chapter is focused on colour imaging, especially colour management.

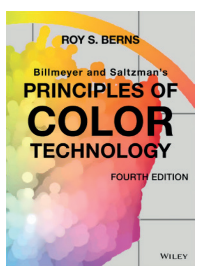

Author: Roy S. Berns

Publisher: Wiley
4th ed., June 2019
ISBN: 978-1-119-36722-2
272 pages
Hardcover
Available also as an eBook

Light Science
Physics and the Visual Arts

Also in the case of this book, which is intended as an introduction to the science of light in a context of art, the new edition was published after 20 years. The text deals with the basic concepts of light and colour, the wave nature of light, ray optics, refraction of light, interference and diffraction, polarised light, light sources and the particle nature of light, sources of colour, colour vision, photography, holography, computer imaging, photonics, visual perception, illusions and the arts. To facilitate an easier understanding of the phenomena of light, the authors provide numerous questions, exercises and about 50 pages describing the experiments for demonstration.

Authors: Thomas Rossing, Christopher J. Chiaverina

Publisher: Springer
2nd ed., January 2020
ISBN: 978-3-030-27102-2
490 pages, 339 images
Hardcover
Available also as an eBook

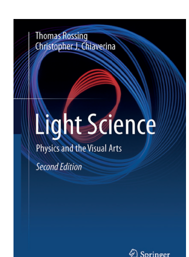

Inclusive Design for a Digital World
Designing with Accessibility in Mind

Considering all kinds of limitations should become natural to each designer of any product so that the highest possible number of people can make use of it. With the present penetration of digital technologies, the accessibility of web content and other user interfaces is an important issue. This book introduces the models of disability and various facets of accessible digital design. It covers the technical aspects, presenting the relevant features of Hypertext Markup Language, Cascading Style Sheets and JavaScript, Accessible Rich Internet Applications (ARIA) specifications and other related web standards, as well as the existing assistive technologies such as the Microsoft Adaptive Controller. The text also discusses the content and design principles, pointing to the importance of a clear structure, correct timing, etc. Design features that are unnecessary or even disturbing usually are not accessible. Further, there are chapters dealing with the research on inclusive design, its planning and implementing, including the approaches to usability testing. The last chapter reviews the innovations and emerging technologies, such as virtual or augmented reality. Although the focus of this text is on the accessibility, the majority of recommendations are valid generally and following them will deliver a better experience to all users.

Author: Regine M. Gilbert

Publisher: Apress
1st ed., December 2019
ISBN: 978-1-4842-5015-0
272 pages, 90 images
Softcover
Available also as an eBook

Graphic Design
A History

With the updated content, including new images and the coverage expanded from the origins of writing to current trends in digital design, the third edition offers also the supplementary material for testing and discussion that is available online. The origins of graphic design are presented in the introduction. The main content is organised into 11 chapters and begins in the 19th century. It continues with the Art Nouveau, German Sachplakat, the First World War, Dada, modern art with Cubism, Futurism, Purism and Art Deco, De Stijl movement and revolution in Russia, the Bauhaus and the New Typography, American modernism and the Second World War, the triumph of the international style, from Swiss Style to its reflections in America, and Postmodernism, up to contemporary graphic design and the digital present.

Author: Stephen J. Eskilson

Publisher: Laurence King Publishing
3rd ed., March 2019
ISBN: 978-1-78627-397-0
472 pages, 550 images
Softcover

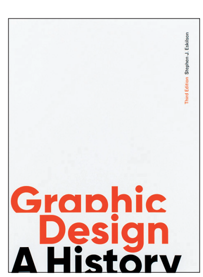

Web Design
The Evolution of the Digital World 1990–Today

Author: Rob Ford
Editor: Julius Wiedemann

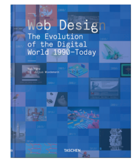

Publisher: Taschen
1st ed., December 2019
ISBN: 978-3836572675
640 pages
Hardcover

After the introductory texts, this volume showcases a selection of the pioneering websites across various categories in the early years from 1990 to 1997 and then by individual years up to 2018, with quotes and insights from their creators. The advances in technology and other key drivers of development, statistics and additional facts are also included.

Paul Rand
Inspiration and Process in Design

Editor: Eugenia Bell

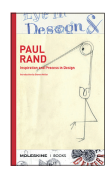

Publisher:
Moleskine Books
1st ed., November 2019
ISBN: 978-1616898595
144 pages
Hardcover

This book presents Paul Rand, an influential American graphic designer, through his drawings from the collection of Steven Heller, who has also written the introduction.

The Art of Graphic Design

Author: Bradbury Thompson

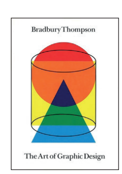

Publisher: Yale University Press
November 2018
ISBN: 978-0300238570
248 pages, 310 images
Softcover

This classic and prised volume by another admired American graphic designer is again available as the 30th-anniversary edition, with a new afterword by Jessica Helfand.

Principles of Lithography

Author: Harry J. Levinson

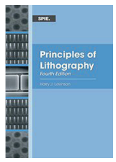

Publisher: SPIE Press
4^{th} ed., May 2019
ISBN: 978-1510627604
630 pages
Hardcover
Also as an eBook

This edition reflects the advances in lithographic technology for chip manufacturing since the third edition of the book published in 2010, especially those connected with extreme ultraviolet (EUV) lithography, which has progressed to the threshold of high-volume manufacturing, and other topics of interest to practising lithographers – line-edge roughness, electron-beam writers and non-linear overlay models. As the book is intended also for the readers unfamiliar with the subject, new problem exercises were added as well.

Sustainable Technologies for Fashion and Textiles

Editor: Rajkishore Nayak

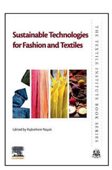

Publisher:
Woodhead Publishing
1^{st} ed., December 2019
ISBN: 978-0081028674
394 pages, Softcover
Also as an eBook

This new book addresses the sustainability issues throughout the supply chain in textile production and processing including printing, garment manufacturing and recycling, while comparing the advantages and disadvantages of different approaches to sustainability. It covers sustainable raw materials, enzyme applications in textile chemical processing, utilisation of ultrasound, plasma and laser technology, recent developments of natural textile colourants and sustainable alternatives to chemicals used in dyeing, printing and finishing operations, sustainable technologies and processes adapted by fashion brands, new approaches in effluent treatment, recycling of textile wastes and also recycling of plastics into textile raw materials.

Advances in Nanostructured Materials and Nanopatterning Technologies
Applications for Healthcare, Environmental and Energy

This volume is written in a compact style and organised into three parts. The first one provides the background, introducing different types of nanocomposite materials with their characteristics and potential use in energy-related, environmental and biomedical applications, as well as the nanofabrication technologies and surface treatments used for their design. Further, it reviews the progress in the bottom-up nanotechnology, enabling fabrication of synthetic molecular devices and machines, and the unconventional subtracting technologies. The second part is dedicated to applications for healthcare. The chapters deal with biomimetic routes to micro- or nanofabrication, nanostructured coatings for antimicrobial applications, advanced organic electroactive nanomaterials for biomedical use and with the utilisation of magnetic nanoparticles for repairing nerve injuries. Six chapters of the third part then review the advances in the area of environment and energy. Namely, this part covers nanostructured electrospun fibres, conductive polymers and metal oxide polymeric composites, light-induced structuring of azopolymer surfaces, nanostructured composite materials for advanced gas sensors, wet-chemistry synthesis of ferro- and ferrimagnetic nanoparticles and also flexible and smart energy harvesters and sensors, with printing techniques described among the additive methods used for their manufacturing.

Editors: Vincenzo Guarino, Maria L. Focarete, Dario Pisignano

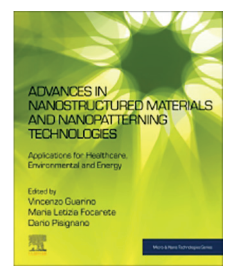

Publisher: Elsevier
1^{st} ed., February 2020
ISBN: 978-0-12-816865-3
472 pages
Softcover
Available also as an eBook

Three-Dimensional Microfabrication Using Two-Photon Polymerization

Four years after the first publication, the current edition brings the content revised with up-to-date information and expanded especially in respect to the materials used in two-photon polymerisation and their chemistry, with the chapters on two-photon photoinitiators for 3D laser microfabrication, materials systems for two-photon lithography and recent advancements in architected mechanical metamaterials, multi-material two-photon polymerisation, etc., as well as the current analytical techniques used to measure and characterise the results of two-photon polymerisation.

Editor: Tommaso Baldacchini

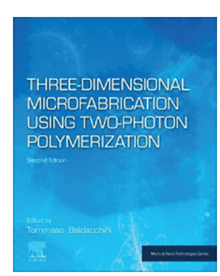

Publisher: William Andrew
2^{nd} ed., October 2019
ISBN: 978-0-12-817827-0
766 pages
Softcover
Available also as an eBook

Bookshelf

Expert reviews

A review of the 2nd edition of Wetting and Spreading Dynamics, the book by Victor M. Starov and Manuel G. Verlade

Book review

Wetting and Spreading Dynamics
2nd edition
Victor M. Starov, Manuel G. Verlade

Reviewed by:
Patrick Gane
School of Chemical Engineering, Department of Bioproducts and Biosystems, Aalto University, Finland

The authors undertake to provide a broad classical résumé of the complex phenomena at play during the interaction of liquids with surfaces. The book is divided into eight sections. The first four sections take the reader from the basics of surface forces and the contact equilibrium between liquid and solid, with focus initially on planar smooth surfaces, through quasi-equilibria as a function of geometry, hysteresis between advancing and receding menisci, leading to kinetics of wetting in terms of thermodynamics, namely heat and mass flow. The remaining sections five through eight increase the complexity of the system by considering porous substrates – the all-important topic for the printer – the role of surfactants and developing the spreading kinetics further to include evaporation. Missing from this otherwise explanatory tour de force is any mention exposing the remaining problems to understanding more fully the discontinuous kinetic phenomena unable to be covered adequately by classical continuity theory.

The second edition elaborates beyond the first edition by including more contemporary research and expanding the collaboration of the authors with numerous internationally active workers in the field. The authors complement each other's knowledge base, spanning the specifics of the surface and physical chemistry of liquids and dispersed systems (Starov) and the overarching physics of nonlinear dynamics and structure on the electronic level (Verlade). Throughout the book the authors care is taken to avoid relying on assumed wisdom, and it is refreshing that such a text is lavishly decorated with terms such as "apparent".

The fundamental theoretical concepts considered

For all material surfaces, the principle of interaction to minimise free energy applies in defining the response to material contact, and that the curvature of a liquid droplet, defining the system pressure via the liquid–vapour interface surface tension, reaches equilibrium with the difference in surface energies of the liquid and contacting surface. An elegant approach is taken to explaining the differences manifest by dispersive and polar surface energy components by considering molecular versus electrostatic forces.

Early in their description of this equilibrium the authors dispel the myth that a direct parallel between surface wetting of rough surfaces can be modelled by the theory of colloidal stability (the Derjaguin–Landau–Vervey–Overbeek (DLVO) theory) by considering the surface geometry alone, but rather the link between geometry and surface forces must be considered. For example, the hysteresis shown between advancing and receding contact angle is neatly explained by considering the fine-scale roughness invisible to the naked eye and the energetic advantage for liquid to remain in a minimal surface free energy state interrupted by the geometry of this roughness creating curvature-related pressure imbalance. The concept recalls nicely the need to consider the isothermal Derjaguin pressure induced by microscopic curvature. Normally, at this point the technician in the field is left to consider only the liquid–surface equilibrium. The authors draw the reader, Book review – continued

Wetting and Spreading Dynamics
2nd edition
Victor M. Starov, Manuel G. Verlade

Reviewed by:
Patrick Gane
School of Chemical Engineering, Department of Bioproducts and Biosystems, Aalto University, Finland

however, into the realisation that the vapour phase in saturation ahead of the wetting front provides an additional attractive force for the liquid to spread across a surface, expressed as negative pressure. Prior to vapour phase saturation the pressure is positive and poses a retarding effect on wetting. Interestingly, variation of the vapour state between saturation and non-saturation, linked also to curvature, can lead to waves being formed in thin films as a quasi-equilibrium state, which can then further develop into depressions in the film.

A short excursion beyond the scope of the book

I take the liberty to diverge here from the text as it is important for the understanding of liquid–pore network interaction, and is a natural advance from the text provided so far. Though not mentioned by the authors, extending the concept of a precursor film pre-empts the likelihood of plug (non-sheared) flow in thin films, which implies also inertial plug flow in very fine pores, typical of coated paper substrates (≤ 0.1 µm), at the start of ink vehicle capillary transport at any point in a pore network wherever a fine pore exits a larger pore. This results in accelerated non-sheared flow into the finest pores first whilst large pores exhibit inertial drag, delaying filling into the larger pores and voids. This breaks with the classical interpretation of Lucas–Washburn viscosity-controlled laminar (Poiseuille) flow. It forms a discontinuity unsolvable by static differential equations at the onset, but can be modelled from a time infinitesimally beyond the start point using the Bosanquet inertial flow model (Schölkopf, J., et al., 2000, Measurement and Network Modelling of Liquid Permeation into Compacted Mineral Blocks, *Journal of Colloid and Interface Science*, 227(1), pp. 119–131; Fries, N. and Dreyer, M., 2008, The transition from inertial to viscous flow in capillary rise, *Journal of Colloid and Interface Science*, 327(1), pp. 125–128).

Following this extension of the material provided in the book is a necessity if the printer is to grasp the reason behind the well-known phenomenon of faster ink setting on fine-pore gloss-coated papers versus large-pore matt-coated papers and uncoated papers, and, in turn, the mechanical properties of the dried print. Thus, the full consideration of the behaviour of liquids on the microscale that is discussed in the book versus nanoscale accelerated interactions missing from the book should encourage the researcher to seek further.

Printing also frequently involves forced wetting, where ink is applied under pressure, e.g. offset blanket contact, onto a semi- or non-wetting surface. Successful ink film transfer is achieved only by the continuity of the cohesive nature of the ink rather than its adhesion to the substrate. Rapid drying and/or polymerisation (UV inks) must be applied to ensure against reticulation (de-wetting), related to the quasi-equilibrium wave phenomenon described earlier in the book as the onset to free menisci development and subsequent de-wetting. Once again such phenomena require the technician in the field to extrapolate from the pure interface science approach followed by the fundamental outline offered in the book.

Further aspects of equilibrium wetting phenomena

Of interest to the printer in the book are the effects developed by a deformable surface, referring both to the substrate to be printed and the printing ink transfer material (e.g. offset blanket). In fact, the deformations discussed in the book provide a fascinating illustration of how printing technology rarely considers the enormous surface tension forces generated as liquid droplets shrink and the menisci retreat during drying on deformable substrates, and how these substrates then become distorted at the print dot level – something of great relevance to large-volume inks with high surface tension, such as are used in inkjet digital non-contact printing. Often wetting in such cases and subsequent substrate deformation are linked purely to cellulose fibre swelling under water contact, but fine structured speciality surfaces can also distort under the capillary and surface tension effects associated with the shrinking droplet.

Coalescence of droplets is a further phenomenon well described in the book, and contrasted with droplet repulsion and deformation when immiscible liquids come into contact – perfectly illustrated in our printer's experience by aqueous fountain solution and oil-based ink side-by-side on a freshly-printed surfaces.

Capillaries and solid surface conjunction/meeting points, such as found in fibrous substrates, acting as capillaries, are well described, but once again the reader must be aware that piqued behaviour in micro capillaries does not provide sufficient explanation for absorption into very fine pore networks, as pointed out above.

An extended theoretical treatment of hysteresis

As the text progresses, the authors return once more to hysteresis and develop the theoretical aspects further. This separation from the earlier geometrical consideration for hysteresis behaviour lies awkwardly in the book, with even redundant repeated diagrams being used. This is the only real case of disjointed writing, but provided the reader remains flexible enough to search throughout the book to complete this topic fully the explanations when joined more than suffice.

Kinetics of wetting

The kinetics of spreading occupies a large part of the remaining pages, and is generally comprehensive, only let down in the short section comparing theory with experiment where the graphical plot axis labels are close to illegible. Nonetheless, a straight line is always convincing even of the observer does not know what it relates to. One does notice the age of the text in respect to the rather poor reproduction quality overall of some graphics. A few hours polishing them would have made the visual experience much more rewarding.

Of great relevance to the printer in this section is the consideration of spreading of a liquid over a thin film of the same liquid. A description of the converse case of different liquids, and the implications for phase separation, are not approached, however, visco-elastic liquids are well described.

Droplets on porous substrates

The important property of droplet behaviour on a porous substrate is discussed, and the impact of lateral pore structure filling advancing beyond the boundaries of the droplet is highlighted. The message is clear – contact angle of a macroscopic droplet on a microporous structured substrate is not a measure of the liquid–solid interaction, i.e. not a measure of surface energy of the solid, but a measure of liquid–liquid contact across a matrix of solid. Furthermore, the book limits the phenomenon of lateral pore structure filling to membranes having pores ≥ 0.2 μm. As mentioned in my

Book review – continued

Wetting and Spreading Dynamics
2nd edition
Victor M. Starov, Manuel G. Verlade

Reviewed by:
Patrick Gane
School of Chemical Engineering, Department of Bioproducts and Biosystems, Aalto University, Finland

Book review – continued

Wetting and Spreading Dynamics
2nd edition
Victor M. Starov, Manuel G. Verlade

Reviewed by:
Patrick Gane
School of Chemical Engineering, Department of Bioproducts and Biosystems, Aalto University, Finland

diversion, fine coated paper has this pore size as a pore volume median with the majority of pores on a number occurrence basis ≤ 0.1 μm, a limit below which plug flow dominates over laminar viscous flow. Similarly, despite fibrous substrates such as uncoated paper having much larger pores, the fibres themselves present continuous internal paper surfaces upon which the initial wetting takes the form of film flow and not one of pore-filling capillary flow. So, once again the theory in the book is limited to the idealised classical case of capillary pressure only.

The presence of surfactants

The role of surfactants is described for enhanced wetting by aqueous liquids on hydrophobic surfaces, and presented mainly through experimental observation of the characteristic two-stage wetting behaviour over time, starting from high contact angle dropping rapidly to the equilibrium value as the wetting line changes from that of liquid–surface contact to that of surfactant mediated wetting. Adsorption of surfactant on the surface is also considered, and the descriptions offered are of high relevance to the printer today facing the change from alcohol surface tension reduction-wetting of fountain solution to surfactant mediated wetting. Given that the book is one of a series dealing with surfactant science, the depth of discussion surrounding them is necessarily detailed, though probably of less interest to the printer than to the surface chemist.

The suggested problems to be solved

The authors conclude their contribution by listing 12 "problems". In fact, they are not problems needing study to improve the science of wetting and spreading but some rather random challenges that might use the science presented. It is suggested by the reviewer that a more useful list could be constructed in respect to the benefits and shortcomings of the classical analytical techniques particularly addressing the discontinuous and nonlinear aspects of accelerating systems, which play the dominant role in industrial and printing applications, such as liquid response to external forces, as mentioned inertial and plug flow phenomena, deviations from laminar flow, cavitation or dissimilar liquid–liquid phase separation. The phenomena under treatise are discontinuous and nonlinear, and so remain poor candidates for equations assuming continuity.

Conclusion

Overall the book is worthy to occupy a prominent place on the technician's bookshelf, and a must for the research scientist starting to understand the complex world sitting at the liquid–substrate–vapour interface, but be ready, nonetheless, not to become complacent in the limited interpretation of that world offered by the carefully chosen timescales and dimensions which fall into classical equilibrium interpretation.

Wetting and Spreading Dynamics

Authors: Victor M. Starov, Manuel G. Velarde
Publisher: CRC Press
2nd ed., July 2019
ISBN: 978-1-138-58407-5
472 pages, 231 images
Hardcover
Available also as an eBook

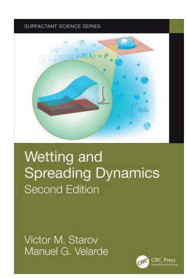

Bookshelf

Academic dissertations

Automation Improvement of Indirect Gravure Printing With a Focus on the Mechanical Characteristics of Silicone Rubber Pads

Doctoral thesis – Summary

Author:
Arash Hakimi Tehrani

Speciality field:
Automation and Measurement

Supervisors:
Edgar Dörsam
Eberhard Abele

Defended:
12 December 2018, Technical University of Darmstadt, Department of Mechanical Engineering, Institute of Printing Science and Technology Darmstadt, Germany

Contact:
arash.hakimi.t@gmail.com

The main concern of this thesis was an improvement in the automation level of the indirect gravure printing process, namely the pad printing that allows printing on 3D objects with uneven surfaces, both concave and convex. While the literature mainly deals with its applications, including functional printing, there is a lack of studies focused on the development of its technology. The research within the presented thesis considered the printing parameters related to the mechanical behaviour of silicone rubber pads in the process with a fixed, stationary substrate and a translational motion of the pad and printing forme. The general aim was to achieve better control over the process and its results, which helps to improve the reliability and repeatability and also to reduce the production costs and waste.

The dissertation outlines the state of the art in the indirect gravure printing including the automation level, presents the characteristics of silicone rubber pads and explains the theoretical equations of hyperelastic materials. One chapter describes the development of the indirect gravure printing machine that comprised the changes in the software, controller, actuators, sensors and mechanic units. The automation level increased from 1 to 3 (on the scale from 0 to 4) thanks to the ability to online monitor the printing process with its parameters and to further process the data. The following part deals with the silicone rubber pads. First, the silicone rubber is characterised by mechanical testing. The dissertation presents the methods and measurement setup along with the test results and selection of the model suitable for simulation. The next chapter describes the steps of pad design from the calculation to production, employing a stereolithographic 3D printer to prepare the pad moulds. Finally, the pad behaviour during printing is simulated using the finite element method (FEM), the results are validated and the contribution to automation level improvement is discussed.

Application of Suspension-Polymerized Latexes in Surface Sizing and Pigment Coating of Paper

Doctoral thesis – Summary

Author:
Araz Rajabi Abhari

Speciality field:
Environmental Materials Science

Supervisor:
Hak Lae Lee

Degree conferral:
26 February 2019, Department of Forest Sciences, Graduate School, Seoul National University Seoul, South Korea

Contact:
araz61@snu.ac.kr

This thesis contributes to the research dealing with the fold cracking of coated papers – the problem that grows with higher amount of filler and heavier coatings being used in papermaking to substitute the use of expensive fibres. The aim was to reduce fold cracking through the improvement of the extensional property and tensile strength of the base paper and coating layer. The approach is based on the use of a suitable surface-sizing additive or paper coating co-binder. In particular, sterically stabilised suspension-polymerised latexes were investigated as an alternative to emulsion-polymerised latexes, which were shown effective in reducing the fold cracking problem but are also connected with foaming issues.

After introducing the background on the suspension-polymerised latexes, surface sizing, coating colour and fold cracking, the dissertation presents three parts of the work that employed the acrylate latexes with a protective shell containing oxidised starch and polyvinyl alcohol. First, the sterically

stabilised suspension-polymerised latex was used as an additive for surface sizing of paper with oxidised starch. It increased the flexibility, tensile strength and internal bond strength of sized papers, with the protective shell improving the formation of hydrogen bonds with starch and base paper. The changes in surface tension and foam generation were also examined. The second part deals with the suspension-polymerised latex used as a co-binder in coating formulation and its effect on the rheological and foaming behaviour. The structure formation of the coating layer influenced by the interaction between the components and resulting surface properties, porosity and optical properties of the coating layer were investigated. The third part is focused on the effect of suspension-polymerised latex co-binder on properties of the coated paper. According to the results, the paper porosity increased with increasing content of suspension-polymerised latex in the coating. The roughness and ink absorption ratio of the coated paper increased as well, while its gloss, brightness and opacity remained almost unchanged. Regarding the mechanical properties of the coated paper, the addition of suspension-polymerised latex slightly enhanced the tensile strength and elongation at break; also, the dry pick resistance was higher. The fold crack area was reduced for both the machine and cross-machine direction in particular in the case of single coated paper.

Doctoral thesis – Summary

Author:
Felipe Clement Fernandes

Speciality field:
Image Acquisition and Image Processing

Supervisors:
Edgar Dörsam
Stefan Katzenbeisser

Defended:
5 June 2019, Technical University of Darmstadt, Department of Mechanical Engineering, Institute of Printing Science and Technology Darmstadt, Germany

Language:
German

Original title:
Entwicklung von gedruckten stochastischen Identifikationsmerkmalen

Contact:
felipe.fernandes@heidelberg.com

Development of Printed Random Identification Features

The aim of this thesis in the area of security elements and anti-counterfeiting technology was to develop a method of printing patterns with stochastic characteristics that can be printed directly onto the print product and identified by means of image processing. The work investigated three types of patterns and employed conventional offset and inkjet printing processes. In all cases, the production of stochastic printed patterns did not require the use of special substrates, inks or machine configurations. The principal research question was whether the stochastic structures produced this way are suitable as an identification feature and if it is possible to optically identify and authenticate them when needed.

The dissertation provides an overview of printing technology, stochastics and physical unclonable functions, generation and description of digital image data, feature extraction using Gabor filtering, Hamming distance, printed identification and security features. Four chapters then describe and discuss the research work conducted within the thesis. For the production of stochastic printed patterns, it was at first needed to define the requirements for these patterns. Most importantly, the pattern must not be predictable from the printed image. Also, the structures should be as fine as possible to provide a high density of information while still enabling optical detection; a sufficient contrast between the structure and the background is also necessary. A pattern with a line-based grid was used for inkjet printing, where the strength of the stochastic effect can be controlled by the line width, line spacing and drop size. For conventional printing, viscous fingering and drip-off print effects were considered. The method of identifying the produced stochastic printed patterns comprised the steps of optical image acquisition, pre-processing, feature extraction and Hamming distance evaluation. Finally, the validation of the method and its further use are presented. For the validation, 270 patterns of each type were processed. The standardised procedure enabled unambiguous identification of the printed patterns of all three types. Repeatability of the method along with the influence of individual processing parameters, transferability of the method and other aspects important for its industrial application are also thoroughly discussed.

Events

Virtual Forum 2020

https://www.flexography.org
22 April & 29 April & 6 May 2020

While the exhibition INFOFLEX 2020 has been cancelled, six technical sessions of the Forum go online and the remaining three will take place later this year at the Fall Conference of the Flexographic Technical Association. Virtual Forum is free for all FTA members and offers the sessions on modern preprint and postprint technologies, press optimisation, colour consistency, the importance of colour to a brand, innovations and student projects.

TAGA Technology & Innovation Series

https://www.taga.org
27–30 April 2020

The Technical Association of the Graphics Arts gives the access to keynote speakers from the cancelled 2020 TAGA Annual Technical Conference (for more details see the Events section in JPMTR 8(2019)4) through this four-day virtual series, which is free also for non-members.

SPIE events

https://spie.org
27 April to 1 May 2020

SPIE Smart Structures + Nondestructive Evaluation Digital Forum 2020

Each SPIE Digital Forum is accessible via the SPIE Digital Library online platform and there is no cost to register. In the case of this one, the programme features e.g. the 22nd Electroactive Polymer Actuators and Devices conference with the study presenting the additive manufacturing of flexible and compact piezoelectric tactile sensors using an inkjet printer and a session dedicated to dielectric elastomer printing. The contributions related to printing technology can be found also in other conferences, such as the one dealing with a diagnostic for droplet characterisation during jetting-based additive manufacturing.

SPIE Defense + Commercial Sensing Digital Forum 2020

This event includes the session on 3D printing for functional and biological applications as a part of the 12th Micro- and Nanotechnology Sensors, Systems, and Applications conference, which also features two invited papers that present the research utilising 3D printing – one for the fabrication of wearable sensor with electrically aligned carbon nanotubes and graphene nanoplatelets and the other for printing conductive traces and antennas while directly attaching silicon dies and components to include chemical sensing in wearable applications.

The events postponed or fully cancelled for 2020

February–March events

From the events presented in this section in JPMTR 8(2019)4, the TAGA Annual Technical Conference and LOPEC 2020 have been cancelled. For several events, new 2020 dates have been announced. These include the WAN-IFRA Newsroom Transformation Programme (28 May to 23 October in three Asian countries), the Asian Media Leaders Summit (21–22 July in Singapore) and Digital Media Europe (10–11 November in Vienna, Austria), as well as FESPA Brasil in São Paulo (23–25 September) and three FESPA events in Madrid, Spain: the Global Print Expo along with the European Sign Expo and Sportswear Pro (6–8 October). Further, the Decorative Surface Conference together with the workshop on Inkjet Technology for Décor Printing has been postponed to 19–21 October (Vienna, Austria). The packaging fair Empack held in Utrecht was at first moved to the end of June and then to 15–17 September. For the Asia Packaging & Printing Industry Expo in Shenzen, China, the new date is still pending.

Another approach has been chosen for SPIE Photonics Europe, which was slightly postponed to 6–10 April and transformed to the Digital Forum, as the other SPIE events impacted by the current pandemic outbreak.

April–June events

Some of the events that should take place in the second quarter of 2020 also have been fully cancelled, with new dates announced for next year. These include PaperCon, the technical conference for the paper and packaging industry organised by TAPPI (25–28 April 2021 in Atlanta, Georgia, USA), the 8th International Symposium on Sensor Science (I3S, 26–28 May 2021 in Dresden, Germany), and the 66th Annual Pulp and Paper Industries Conference (20–24 June 2021 in Niagara Falls, Ontario, Canada). Another cancelled event is the 33rd International Publishers Congress of the International Publishers Association with the Norwegian Publishers Association planned for 28–30 May 2020 in Lillehammer, Norway; the new date has not been set.

However, the event that seems to find the right date with the most difficulty is drupa, which was at first announced for 2019. Then it was decided to keep a four-year cycle and the fair was scheduled from 23 June to 3 July 2020, which was later moved a week earlier to 16–26 June 2020. Now the date had to be postponed again. The next drupa should be held in Düsseldorf on 20–30 April 2021.

Several events originally scheduled for the coming weeks and months have been postponed to the new dates later in 2020. As the first one of these, the 5th CIE Expert Symposium on Colour and Visual Appearance should be held in Hong Kong on 27–29 July. On 16–19 August, the International Conference on Flexible and Printable Sensors and Systems, IEEE FLEPS 2020, is announced to be held in Manchester, UK. The events rescheduled for September include the Future Manufacturing Technologies Conference (FMTX, 16 September in Copenhagen, Denmark), the 12th 3D Printing Days (22–24 September in Kielce, Poland) and the London Imaging Meeting, a new conference jointly organised by the Society for Imaging Science and the Technology and Printing and Graphics Science Group of the Institute of Physics (30 September to 1 October in London, UK).

Considering the evolving situation, these dates are tentative; we hope to bring the updated information in the summer issue, JPMTR 9(2020)2. It should cover also the other events postponed without announcing new dates, such as the Inkjet Ink Characterisation Practical Course in Hamburg, Germany, the Printed Electronics Europe in Berlin, Germany, and the CPES2020 conference in Brampton, Ontario, Canada.

INMA (Virtual) World Congress

https://www.inma.org
5–28 May 2020

After cancelling the World Congress of News Media, the International News Media Association organises this virtual event, which includes nine modules scheduled during May. With a claim ‘Re-Thinking News Media in the Age of Coronavirus’, the topics cover subscription experiences, advertising, smart data, the so-called content to commerce, building brand and community, inspiring ideas and stories of innovation, framed with a discussion where news media goes next and the 2021 outlook.

Archiving

http://www.imaging.org
18–21 May 2020

The online Archiving Short Courses are scheduled for 7–15 May, with the course recordings available online until 15 July 2020. The four-day conference programme then offers, for example, the keynote talk by Roy S. Berns, discussing the obstacles and opportunities connected with the use of spectral imaging systems for archiving purposes.

12th International Conference on Hybrid and Organic Photovoltaics

https://www.nanoge.org
25–28 May 2020

The HOPV20 Online Conference consists of four symposia on perovskite fundamentals, characterisation methods, perovskite applications and organic solar cells. Each day, the invited talks are followed by the ePoster session, with an opportunity to discuss through a chatroom.

Webinar events

The webinar series scheduled for the coming weeks include the free Enfocus Virtual Safari 2020 on Thursdays in April and May, with the webinars covering prepress automation, on-demand book printing, standardisation in print, specific software solutions, etc. On Mondays from 27 April to 18 May, Fogra offers free “taster” courses of the new one-year Fogra Web Academy (starting from 7 September 2020). The topics are multicolour printing, international standardisation for the printing industry, process parameters in offset printing and ICC profile making. Many webinars that reflect the current situation in news publishing are organised by the World Association of News Publishers, WAN-IFRA. Similarly, the webinar ‘COVID-19: The path forward for the economy and print markets’ is offered on 23 April by Printing Industries of America. Its Sales Ready! 2020 virtual conference is scheduled for 4–8 May.

A traditional event currently transformed into a webinar format is the CreativePro Week 2020 held by the CreativePro Network. It takes place as an online event (1–5 June), including the Print & ePublishing Conference PePcon.

Journal of
Print and Media Technology
Research
A PEER-REVIEWED QUARTERLY

ISSN 2414-6250 (Online)
ISSN 2223-8905 (Print)
CODEN JPMTBI
UDC 665

Call for papers

The Journal of Print and Media Technology Research is a peer-reviewed periodical, published quarterly by iarigai, the International Association of Research Organizations for the Information, Media and Graphic Arts Industries.

JPMTR is listed in Emerging Sources Citation Index, Scopus, Index Copernicus International, PiraBase (by Smithers Pira), Paperbase (by Innventia and Centre Technique du Papier), NSD – Norwegian Register for Scientific Journals, Series and Publishers.

Authors are invited to prepare and submit complete, previously unpublished and original works, which are not under review in any other journals and/or conferences.

The journal will consider for publication papers on fundamental and applied aspects of at least, but not limited to, the following topics:

- **Printing technology and related processes**
  Conventional and special printing; Packaging; Fuel cells, batteries, sensors and other printed functionality; Printing on biomaterials; Textile and fabric printing; Printed decorations; 3D printing; Material science; Process control

- **Premedia technology and processes**
  Colour reproduction and colour management; Image and reproduction quality; Image carriers (physical and virtual); Workflow and management

- **Emerging media and future trends**
  Media industry developments; Developing media communications value systems; Online and mobile media development; Cross-media publishing

- **Social impact**
  Environmental issues and sustainability; Consumer perception and media use; Social trends and their impact on media

Submissions for the journal are accepted at any time. If meeting the general criteria and ethic standards of scientific publishing, they will be rapidly forwarded to peer-review by experts of relevant scientific competence, carefully evaluated, selected and edited. Once accepted and edited, the papers will be published as soon as possible.

There is no entry or publishing fee for authors. Authors of accepted contributions will be asked to sign a copyright transfer agreement.

Authors are asked to strictly follow the guidelines for preparation of a paper (see the abbreviated version on inside back cover of the journal).

Complete guidelines can be downloaded from: <http://www.iarigai.org/publications/journals/>
Papers not complying with the guidelines will be returned to authors for revision.

Submissions and queries should be directed to: journal@iarigai.org

Journal of
Print and Media Technology Research
A PEER-REVIEWED QUARTERLY

Vol. 9, 2020

Prices and subscriptions

Since 2016, the journal is published in digital form; current and archive issues are available at: <https://iarigai.com/publications/journals/>.

Since 2020, the journal will be published as "open access" publication, available free of charge for iarigai members, subscribers, authors, contributors and all other interested public users.

A print version is available on-demand. Please, find below the prices charged for the printed Journal, for four issues per year as well as for a single issue

Regular prices

Four issues, print JPMTR (on-demand)	400 EUR
Single issue, print JPMTR (on-demand)	100 EUR

Subscription prices

Annual subscription, four issues, print JPMTR (on-demand)	400 EUR

Prices for iarigai members

Four issues, print JPMTR (on-demand)	400 EUR
Single issue, print JPMTR (on-demand)	100 EUR

Place your order online at: <http://www.iarigai.org/publications/subscriptions-orders/>
Or send an e-mail order to: office@iarigai.org

Guidelines for authors

Authors are encouraged to submit complete, original and previously unpublished scientific or technical research works, which are not under reviews in any other journals and/or conferences. Significantly expanded and updated versions of conference presentations may also be considered for publication. In addition, the Journal will publish reviews as well as opinions and reflections in a special section.

Submissions for the journal are accepted at any time. If meeting the general criteria and ethical standards of the scientific publication, they will be rapidly forwarded to peer-review by experts of high scientific competence, carefully evaluated, and considered for selection. Once accepted by the Editorial Board, the papers will be edited and published as soon as possible.

When preparing a manuscript for JPMTR, please strictly comply with the journal guidelines. The Editorial Board retains the right to reject without comment or explanation manuscripts that are not prepared in accordance with these guidelines and/or if the appropriate level required for scientific publishing cannot be attained.

A – General

The text should be cohesive, logically organized, and thus easy to follow by someone with common knowledge in the field. Do not include information that is not relevant to your research question(s) stated in the introduction.

Only contributions submitted in English will be considered for publication. If English is not your native language, please arrange for the text to be reviewed by a technical editor with skills in English and scientific communications. Maintain a consistent style with regard to spelling (either UK or US English, but never both), punctuation, nomenclature, symbols etc. Make sure that you are using proper English scientific terms. Literal translations are often wrong. Terms that do not have a commonly known English translation should be explicitly defined in the manuscript. Acronyms and abbreviations used must also be explicitly defined. Generally, sentences should not be very long and their structure should be relatively simple, with the subject located close to its verb. Do not overuse passive constructions.

Do not copy substantial parts of your previous publications and do not submit the same manuscript to more than one journal at a time. Clearly distinguish your original results and ideas from those of other authors and from your earlier publications – provide citations whenever relevant.

For more details on ethics in scientific publication consult Guidelines, published by the Committee on Publication Ethics (COPE):
<https://publicationethics.org/resources/guidelines>

If it is necessary to use an illustration, diagram, etc. from an earlier publication, it is the author's responsibility to ensure that permission to reproduce such an illustration, diagram, etc. is obtained from the copyright holder. If a figure is copied, adapted or redrawn, the original source must be acknowledged.

Submitting the contribution to JPMTR, the author(s) confirm that it has not been published previously, that it is not under consideration for publication elsewhere and – once accepted and published – it will not be published under the same title and in the same form, in English or in any other language. The published paper may, however, be republished as part of an academic thesis to be defended by the author. The publisher retains the right to publish the printed paper online in the electronic form and to distribute and market the Journal containing the respective paper without any limitations.

B – Structure of the manuscript

Preliminary

Title: Should be concise and unambiguous, and must reflect the contents of the article. Information given in the title does not need to be repeated in the abstract (as they are always published jointly), although some overlap is unavoidable.

List of authors: I.e. all persons who contributed substantially to study planning, experimental work, data collection or interpretation of results and wrote or critically revised the manuscript and approved its final version. Enter full names (first and last), followed by the present address, as well as the E-mail addresses. Separately enter complete details of the corresponding author – full mailing address, telephone number, and E-mail. Editors will communicate only with the corresponding author.

Abstract: Should not exceed 500 words. Briefly explain why you conducted the research (background), what question(s) you answer (objectives), how you performed the research (methods), what you found (results: major data, relationships), and your interpretation and main consequences of your findings (discussion, conclusions). The abstract must reflect the content of the article, including all keywords, as for most readers it will be the major source of information about your research. Make sure that all the information given in the abstract also appears in the main body of the article.

Keywords: Include three to five relevant scientific terms that are not mentioned in the title. Keep the keywords specific. Avoid more general and/or descriptive terms, unless your research has strong interdisciplinary significance.

Scientific content

Introduction and background: Explain why it was necessary to carry out the research and the specific research question(s) you will answer. Start from more general issues and gradually focus on your research question(s). Describe relevant earlier research in the area and how your work is related to this.

Methods: Describe in detail how the research was carried out (e.g. study area, data collection, criteria, origin of analyzed material, sample size, number of measurements, equipment, data analysis, statistical methods and software used). All factors that could have affected the results need to be considered. Make sure that you comply with the ethical standards, with respect to the environmental protection, other authors and their published works, etc.

Results: Present the new results of your research (previously published data should not be included in this section). All tables and figures must be mentioned in the main body of the article, in the order in which they appear. Make sure that the statistical analysis is appropriate. Do not fabricate or distort any data, and do not exclude any important data; similarly, do not manipulate images to make a false impression on readers.

Discussion: Answer your research questions (stated at the end of the introduction) and compare your new results with published data, as objectively as possible. Discuss their limitations and highlight your main findings. At the end of Discussion or in a separate section, emphasize your major conclusions, pointing out scientific contribution and the practical significance of your study.

Conclusions: The main conclusions emerging from the study should be briefly presented or listed in this section, with the reference to the aims of the research and/or questions mentioned in the Introduction and elaborated in the Discussion.

Note: Some papers might require different structure of the scientific content. In such cases, however, it is necessary to clearly name and mark the appropriate sections, or to consult the editors. Sections from Introduction until the end of Conclusions must be numbered. Number the section titles consecutively as 1., 2., 3., ... while subsections should be hierarchically numbered as 2.1, 2.3, 3.4 etc. Only Arabic numerals will be accepted.

Acknowledgments: Place any acknowledgements at the end of your manuscript, after conclusions and before the list of literature references.

References: The list of sources referred to in the text should be collected in alphabetical order on at the end of the paper. Make sure that you have provided sources for all important information extracted from other publications. References should be given only to documents which any reader can reasonably be expected to be able to find in the open literature or on the web, and the reference should be complete, so that it is possible for the reader to locate the source without difficulty. The number of cited works should not be excessive - do not give many similar examples.

Responsibility for the accuracy of bibliographic citations lies entirely with the authors. Please use exclusively the Harvard Referencing System. For more information consult the Guide to Harvard style of Referencing, 6th edition, 2019, used with consent of Anglia Ruskin University, available at:
<https://libweb.anglia.ac.uk/referencing/files/Harvard_referencing_201718.pdf>

C – Technical requirements for text processing

For technical requirement related to your submission, i.e. page layout, formatting of the text, as well of graphic objects (images, charts, tables etc.) please see detailed instructions at:
<http://www.iarigai.org/publications/journals/>

D – Submission of the paper and further procedure

Before sending your paper, check once again that it corresponds to the requirements explicated above, with special regard to the ethical issues, structure of the paper as well as formatting.

Once completed, send your paper as an attachment to:
journal@iarigai.org

If necessary, compress the file before sending it. You will be acknowledged on the receipt within 48 hours, along with the code under which your submission will be processed.

The editors will check the manuscript and inform you whether it has to be updated regarding the structure and formatting. The corrected manuscript is expected within 15 days.

Your paper will be forwarded for anonymous evaluation by two experts of international reputation in your specific field. Their comments and remarks will be in due time disclosed to the author(s), with the request for changes, explanations or corrections (if any) as demanded by the referees.

After the updated version is approved by the reviewers, the Editorial Board will decide on the publishing of the paper. However, the Board retains the right to ask for a third independent opinion, or to definitely reject the contribution.

Printing and publishing of papers, once accepted by the Editorial Board, will be carried out at the earliest possible convenience.

1-2020

Journal of
Print and Media Technology Research
A PEER-REVIEWED QUARTERLY

The journal is publishing contributions in the following fields of research

- Printing technology and related processes
- Premedia technology and processes
- Emerging media and future trends
- Social impacts

For details see the Mission statement inside

JPMTR is listed in

- Emerging Sources Citation Index
- Scopus
- Index Copernicus International
- PiraBase (by Smithers Pira)
- Paperbase (by Innventia and Centre Technique du Papier)
- NSD – Norwegian Register for Scientific Journals, Series and Publishers

Submissions and inquiries

journal@iarigai.org

Subscriptions

office@iarigai.org

More information at

www.iarigai.org/publications/journal

Publisher

The International Association of Research Organizations
for the Information, Media and Graphic Arts Industries
Magdalenenstrasse 2
D-64288 Darmstadt
Germany